Annu. Rev. Fluid Mech. 1994. 26 : 23–63

LAGRANGIAN PDF METHODS FOR TURBULENT FLOWS

S. B. Pope

Sibley School of Mechanical and Aerospace Engineering,
Cornell University, Ithaca, New York 14853

KEY WORDS: turbulence modeling, stochastic methods, Langevin equation

1. INTRODUCTION

Lagrangian Probability Density Function (PDF) methods have arisen in the past 10 years as a union between PDF methods and stochastic Lagrangian models, similar to those that have long been used to study turbulent dispersion. The methods provide a computationally-tractable way of calculating the statistics of inhomogeneous turbulent flows of practical importance, and are particularly attractive if chemical reactions are involved. The information contained at this level of closure—equivalent to a multi-time Lagrangian joint pdf—is considerably more than that provided by moment closures.

The computational implementation is conceptually simple and natural. At a given time, the turbulent flow is represented by a large number of particles, each having its own set of properties—position, velocity, composition etc. These properties evolve in time according to stochastic model equations, so that the computational particles simulate fluid particles. The particle-property time series contain information equivalent to the multi-time Lagrangian joint pdf. But, at a fixed time, the ensemble of particle properties contains no multi-point information: Each particle can be considered to be sampled from a different realization of the flow. (Hence two particles can have the same position, but different velocities and compositions.)

It is generally acknowledged (e.g. Reynolds 1990) that many different approaches have important roles to play in tackling the problems posed by turbulent flows. Each approach has its own strengths and weaknesses.

0066–4189/94/0115–0023$05.00

At one end of the spectrum of approaches, Direct Numerical Simulations (DNS) offer unmatched accuracy, but their computational cost is high, and their range of applicability is extremely limited (Reynolds 1990). At the other end of the spectrum, simple turbulence models such as k-ε (Launder & Spalding 1972) offer essentially unrestricted applicability, moderate cost, but poor or uncertain accuracy (except in some simple flows). Compared to such turbulence models, Lagrangian PDF methods have the same wide applicability; their cost is greater (but less than DNS); and, for the reasons presented below, their potential for accuracy is greatly increased.

In going beyond simple turbulence models (i.e. moment closures), the challenge is to incorporate a fuller description of the turbulence, while retaining computational tractability. If appropriately chosen, the fuller description allows unsatisfactory modeling assumptions to be avoided, and at the same time provides more information to model the unavoidable.

It can be argued that the dominant process in turbulent flows is convection (by the instantaneous fluid velocity). At high Reynolds number, molecular diffusion makes a negligible contribution to spatial transport, and so convection dominates the transport of momentum, chemical species, and enthalpy. In moment closures, at some level, convection is modeled by a gradient diffusion assumption, which can lead to qualitatively incorrect behavior (see, for example, Deardorff 1978). In Lagrangian PDF methods, on the other hand, convection is treated simply and naturally in the Lagrangian frame with no modeling assumptions. Similarly, in reacting flows, finite-rate nonlinear reaction rates can present insurmountable difficulties to moment closures; whereas arbitrarily complex reactions can be handled naturally by Lagrangian PDF methods, without modeling assumptions (Pope 1985, 1990).

In any statistical approach to turbulence, modeling assumptions are required at some level. It is notoriously difficult to construct general and accurate models for turbulence, whereas there are many other stochastic physical phenomena for which simple statistical models are successful (see e.g. van Kampen 1983). There are two features of turbulent flows that go a long way to explaining the inherent difficulties. First, turbulence has a long memory: In free shear flows, it is readily deduced (from experimental data) that the characteristic time scale of the energy-containing turbulent motion is, typically, four times the characteristic mean-flow time scale. Second, through the fluctuating pressure field, the velocity field experiences long-range interactions. Among other effects, this can lead to large-scale organized motions, and to the boundary geometry influencing the turbulence structure in the interior of the flow.

Lagrangian PDF methods can take full account of the long memory of

turbulence. For the fluid properties considered, the multi-time Lagrangian joint pdf completely describes the past history of all fluid particles that (on different realizations) pass through a given point at a given time. As discussed in Section 5, the long-memory incorporated in current stochastic Lagrangian models leads to fluid-particle motions that are consistent with large-scale turbulent structures.

In the next Section the relevant Eulerian and Lagrangian pdfs are introduced, and the different PDF methods are categorized. Section 3 is devoted to the Langevin equation. This equation provides a simple stochastic model for the velocity of a fluid particle: It is also a building block for other stochastic models. The particle representation of a turbulent flow, which is fundamental to the Lagrangian PDF approach, is described in Section 4. Then more recent and sophisticated stochastic models are reviewed in Section 5.

2. EULERIAN AND LAGRANGIAN PDF METHODS

The purpose of this section is to introduce the various pdfs considered, to categorize PDF methods, and to provide references to the relevant literature.

2.1 *Eulerian pdfs*

We start by considering a single *composition variable* (e.g. a species mass fraction) which, at position $\mathbf{x}$ and time t, is denoted by $\phi(\mathbf{x}, t)$. At fixed $(\mathbf{x}, t)$, ϕ is a random variable, corresponding to which we introduce the independent *sample-space variable* ψ. Then the *cumulative distribution function* (cdf) of ϕ is defined by

$$F_\phi(\psi, \mathbf{x}, t) \equiv \text{Prob}\,\{\phi(\mathbf{x}, t) < \psi\}, \tag{1}$$

and the *probability density function* (pdf) of ϕ is

$$f_\phi(\psi; \mathbf{x}, t) \equiv \frac{\partial}{\partial \psi} F_\phi(\psi, \mathbf{x}, t). \tag{2}$$

The fundamental significance of the pdf is that it measures the probability of the random variable being in any specified interval. For example, for $\psi_b > \psi_a$, from Equations (1) and (2) we obtain

$$\text{Prob}\,\{\psi_a \le \phi(\mathbf{x}, t) < \psi_b\} = \int_{\psi_a}^{\psi_b} f_\phi(\psi; \mathbf{x}, t)\, d\psi. \tag{3}$$

The pdf just defined, $f_\phi(\mathbf{x}, t)$, is the one-point, one-time Eulerian pdf of $\phi(\mathbf{x}, t)$. It completely describes the random variable ϕ at each $\mathbf{x}$ and t

separately; but it contains no joint information about ϕ at two or more space-time points. If $\phi(\mathbf{x}, t)$ is statistically homogeneous, then f_ϕ is independent of $\mathbf{x}$.

More generally, we may want to consider a set of σ composition variables $\boldsymbol{\phi}(\mathbf{x}, t)$ where $\boldsymbol{\phi} = \{\phi_1, \phi_2, \ldots, \phi_\sigma\}$. Then, with $\boldsymbol{\psi} = \{\psi_1, \psi_2, \ldots, \psi_\sigma\}$ being corresponding sample-space variables, the joint pdf of $\boldsymbol{\phi}$ is denoted by $f_{\boldsymbol{\phi}}(\boldsymbol{\psi}; \mathbf{x}, t)$. Further, with $\mathbf{U}(\mathbf{x}, t)$ being the Eulerian velocity of the fluid, we introduce sample-space velocity variables $\mathbf{V} = \{V_1, V_2, V_3\}$ and denote the (one-point, one-time Eulerian) joint pdf of velocity by $f_{\mathbf{u}}(\mathbf{V}; \mathbf{x}, t)$. Finally, the velocity-composition joint pdf is denoted by $f(\mathbf{V}, \boldsymbol{\psi}; \mathbf{x}, t)$.

By definition, *in a PDF method, a pdf (or joint pdf) in a turbulent flow is determined as the solution of a modeled evolution equation.*

2.2 *Assumed PDF Methods*

In spite of their name, *assumed PDF methods* are not PDF methods (according to the above definition). Instead of being determined from a modeled evolution equation, the pdf is assumed to have a particular shape that is parametrized (usually) by its first and second moments. The method has found application in combustion (e.g. Bilger 1980). For the pdf of a single composition, the suggested shapes include: a beta-function distribution (Rhodes 1975); a clipped Gaussian (Lockwood & Naguib 1975); and a maximum entropy distribution (Pope 1980). The extension to several composition variables, which is considerably more difficult, has been considered by, among others, Correa et al (1984), Bockhorn (1990), and Girimaji (1991).

Although assumed PDF methods are favored in some applications, compared to PDF methods they have two disadvantages. First, no account is taken of the influence of the dynamics (e.g. reaction) on the shape of the pdf. Second—and maybe surprising at first sight—assumed PDF methods are computationally more expensive (if not intractable) for the general case of many compositions.

2.3 *Eulerian PDF Methods*

One of the first cases studied using PDF methods, and one that continues to receive considerable attention, is reaction in constant-density homogeneous turbulence. In the simplest situation, the composition is characterized by a single passive scalar $\phi(\mathbf{x}, t)$, that evolves by

$$\frac{D\phi}{Dt} = \Gamma \nabla^2 \phi + S(\mathbf{x}, t). \tag{4}$$

Here $D/Dt = \partial/\partial t + \mathbf{U} \cdot \nabla$ is the substantial derivative, Γ is the (constant)

molecular diffusivity, and the reaction rate is a known function of the composition:

$$S(\mathbf{x}, t) = \hat{S}[\phi(\mathbf{x}, t)]. \tag{5}$$

For the statistically homogeneous case considered, the composition pdf $f_\phi(\psi; t)$ is independent of $\mathbf{x}$. Without further assumption, the evolution equation for f_ϕ can be deduced from Equation (4). This can be done using any one of several different techniques that have been developed over the years. These techniques are reviewed by Pope (1985), Dopazo (1993), and Kuznetsov & Sabel'nikov (1990), and are not described here. For the present case the result for $f_\phi(\psi; t)$ is

$$\frac{\partial}{\partial t} f_\phi = -\frac{\partial^2}{\partial \psi^2}[f_\phi \chi(\psi, t)] - \frac{\partial}{\partial \psi}[f_\phi \hat{S}(\psi)], \tag{6}$$

where

$$\chi(\psi, t) \equiv \Gamma \langle \nabla \phi \cdot \nabla \phi | \phi(\mathbf{x}, t) = \psi \rangle \tag{7}$$

is the conditional scalar dissipation.

An important observation is that the reaction term in the pdf equation (6) is in closed form, whereas the corresponding terms in moment closures [e.g. $\langle \hat{S}(\phi) \rangle$ and $\langle \phi \hat{S}(\phi) \rangle$] are not—hence the attraction of PDF methods for reactive flows.

The term involving χ in Equation (6) represents molecular mixing and requires modeling. In general—as exemplified by Equation (7)—*in Eulerian PDF methods, the quantities that have to be modeled are one-point one-time conditional expectations.*

Molecular mixing models (which model the term in χ in Equation 6) have a long history which is briefly reviewed in Section 5.5 and more thoroughly elsewhere (Pope 1982, 1985; Borghi 1988; Dopazo 1993); and there are several relevant recent works (Chen et al 1989, Sinai & Yakhot 1989, Valiño & Dopazo 1991, Pope 1991a, Gao 1991, Gao & O'Brien 1991, Fox 1992, Pope & Ching 1993).

The composition PDF method can be extended to several compositions, and to inhomogeneous flows. The latter necessitates modeling turbulent convection—generally as gradient diffusion. Recent applications to multi-dimensional flows are described by Chen et al (1990), Roekaerts (1991), and Hsu et al (1993).

For inhomogeneous flows, the method based on the velocity-composition joint pdf $f(\mathbf{V}, \boldsymbol{\psi}; \mathbf{x}, t)$ has the advantage of avoiding gradient-diffusion modeling. For constant-density flow, the Navier-Stokes equations can be written

$$\frac{D\mathbf{U}}{Dt} = \nu\nabla^2\mathbf{U} - \nabla\langle p\rangle - \nabla p', \tag{8}$$

where ν is the kinematic viscosity, and the pressure (divided by the density) p is subjected to the Reynolds decomposition. From this equation, and from Equation (4) written for each composition $\phi_\alpha(\mathbf{x}, t)$, the evolution equation for $f(\mathbf{V}, \boldsymbol{\psi}; \mathbf{x}, t)$ can be deduced to be

$$\frac{\partial f}{\partial t} + V_i\frac{\partial f}{\partial x_i} + \frac{\partial}{\partial \psi_\alpha}[f\hat{S}_\alpha(\psi)] - \frac{\partial\langle p\rangle}{\partial x_i}\frac{\partial f}{\partial V_i} = \frac{\partial}{\partial V_i}\left[f\left\langle\frac{\partial p'}{\partial x_i} - \nu\nabla^2 U_i|\mathbf{V}, \boldsymbol{\psi}\right\rangle\right] - \frac{\partial}{\partial \psi_\alpha}[f\langle\Gamma\nabla^2\phi_\alpha|\mathbf{V}, \boldsymbol{\psi}\rangle], \tag{9}$$

where $\langle\nabla^2\phi_\alpha|\mathbf{V}, \boldsymbol{\psi}\rangle$ is written for the conditional expectation $\langle\nabla^2\phi_\alpha|\mathbf{U}(\mathbf{x}, t) = \mathbf{V}, \boldsymbol{\phi}(\mathbf{x}, t) = \boldsymbol{\psi}\rangle$, and the summation convention applies to α as well as to i.

The terms on the left-hand side of Equation (9) are in closed form and represent convection, reaction, and acceleration due to the mean pressure gradient. Those on the right-hand side contain one-point one-time conditional expectations. Models for the effects of the viscous stresses and the fluctuating pressure gradient are discussed below.

2.4 *Lagrangian pdfs*

Fundamental to the Lagrangian description is the notion of a *fluid particle*. Let t_0 be a reference time, and let $\mathbf{x}_0 = \{x_{01}, x_{02}, x_{03}\}$ be *Lagrangian coordinates*. Then $\mathbf{x}^+(t, \mathbf{x}_0)$ denotes the position at time t of the fluid particle that is at $\mathbf{x}_0$ at time t_0 [i.e. $\mathbf{x}^+(t_0, \mathbf{x}_0) = \mathbf{x}_0$].

For each Eulerian variable [e.g. $\mathbf{U}(\mathbf{x}, t)$] the corresponding Lagrangian variable (denoted by the superscript $+$) is defined by (for example)

$$\mathbf{U}^+(t, \mathbf{x}_0) = \mathbf{U}[\mathbf{x}^+(t, \mathbf{x}_0), t]. \tag{10}$$

By definition, a fluid particle moves with its own velocity. So, given the Eulerian velocity, $\mathbf{x}^+$ is determined as the solution of

$$\frac{\partial\mathbf{x}^+(t, \mathbf{x}_0)}{\partial t} = \mathbf{U}^+(t, \mathbf{x}_0), \tag{11}$$

with the initial condition

$$\mathbf{x}^+(t_0, \mathbf{x}_0) = \mathbf{x}_0. \tag{12}$$

To simplify the subsequent development we impose two restrictions. First, we consider flow domains that are (possibly time-dependent) material volumes. Thus fluid particles do not cross the boundary of the

flow domain. Second, we consider constant-density flow so that the determinant of the Jacobian $\partial x_i^+/\partial x_{0j}$ is unity. Both of these restrictions are readily removed (see Pope 1985).

The primary Lagrangian pdf considered is

$$f_{\mathrm{L}}(\mathbf{V}, \mathbf{x}; t|\mathbf{V}_0, \mathbf{x}_0), \tag{13}$$

which is the joint pdf of the event

$$\{\mathbf{U}^+(t, \mathbf{x}_0) = \mathbf{V}, \mathbf{x}^+(t, \mathbf{x}_0) = \mathbf{x}\} \tag{14}$$

subject to the condition $\mathbf{U}^+(t_0, \mathbf{x}_0) = \mathbf{V}_0$. Thus f_{L} is the joint pdf of the fluid particle properties at time t, conditional upon their properties at time t_0. Note that, in the Lagrangian pdf f_{L}, $\mathbf{x}$ denotes the sample space corresponding to $\mathbf{x}^+(t, \mathbf{x}_0)$, while in the Eulerian pdf it is a parameter. Also, other fluid particle properties [e.g. $\boldsymbol{\phi}^+(t, \mathbf{x}_0)$] can be included in the definition of f_{L}.

The Lagrangian pdf f_{L} is defined in terms of the reference initial time t_0 and a future time $t > t_0$. More generally, we may consider M times $t_0 < t_1 < t_2 \ldots < t_M$, and define the M-time Lagrangian pdf

$$f_{\mathrm{LM}}(\mathbf{V}_M, \mathbf{x}_M; t_m; \mathbf{V}_{M-1}, \mathbf{x}_{M-1}; t_{M-1}; \ldots; \mathbf{V}_1, \mathbf{x}_1; t_1|\mathbf{V}_0, \mathbf{x}_0) \tag{15}$$

as the joint pdf of the events

$$\{\mathbf{U}^+(t_k, \mathbf{x}_0) = \mathbf{V}_k, \mathbf{x}^+(t_k, \mathbf{x}_0) = \mathbf{x}_k; k = 1, 2, \ldots, M\} \tag{16}$$

subject to the same initial condition as before, $\mathbf{U}^+(t_0, \mathbf{x}_0) = \mathbf{V}_0$.

2.5 *Lagrangian PDF Methods*

In Eulerian PDF methods, the quantities to be modeled are one-point, one-time conditional expectations (see Equation 9). In Lagrangian PDF methods, the modeling approach is entirely different. Stochastic models are constructed to simulate the evolution of fluid particle properties. For example, Figure 1 shows the time series of one component of velocity (in stationary, homogeneous, isotropic turbulence) according to a simple stochastic model—the Langevin equation (which is the subject of the next Section).

It is useful to distinguish between the fluid-particle properties ($\mathbf{U}^+$ and $\mathbf{x}^+$) and the values obtained from the stochastic models. Thus $\mathbf{U}^*(t)$ and $\mathbf{x}^*(t)$ denote the modeled particle properties, with $\mathbf{x}^*$ evolving by

$$\frac{d\mathbf{x}^*(t)}{dt} = \mathbf{U}^*(t). \tag{17}$$

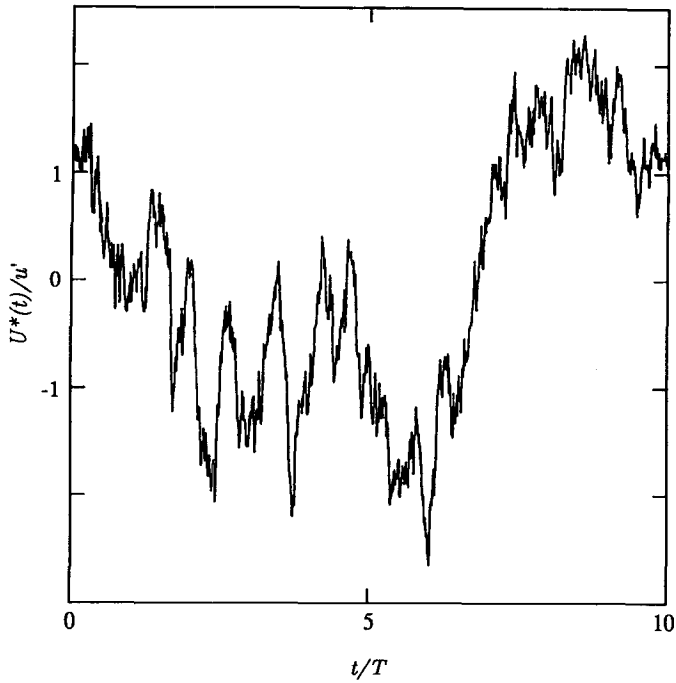

Figure 1 Sample of an Ornstein-Uhlenbeck process obtained as the solution of the Langevin equation (Equation 21).

Then $f_L^*(\mathbf{V}, \mathbf{x}; t|\mathbf{V}_0, \mathbf{x}_0)$ is the joint pdf to $\mathbf{U}^*(t)$ and $\mathbf{x}^*(t)$ subject to the initial condition

$$\mathbf{U}^*(t_0) = \mathbf{V}_0, \mathbf{x}^*(t_0) = \mathbf{x}_0. \tag{18}$$

If the stochastic model is accurate, then f_L^* is an accurate approximation to f_L.

Stochastic Lagrangian models—such as the Langevin equation—have long been used in studies of turbulent dispersion, where the quantities of interest are (or can be obtained from) Lagrangian pdfs. For example, if a pulse of a contaminant is released at time t_0 and location $\mathbf{x}_0$, then (if molecular diffusion can be neglected) the expected concentration of the contaminant at a later time t is proportional to the pdf of $\mathbf{x}^+(t, \mathbf{x}_0)$, which is modeled by $\mathbf{x}^*(t)$. In fact, as early as 1921, G. I. Taylor proposed a stochastic model for $\mathbf{x}^*(t)$ precisely for this application (Taylor 1921).

A direct numerical implementation of a stochastic model of turbulent dispersion is to release a large number N of particles at the source [i.e. $\mathbf{x}^*(t_0) = \mathbf{x}_0$] with initial velocities $\mathbf{U}^*(t_0)$ distributed according to the Eulerian pdf $f(\mathbf{V}; \mathbf{x}_0, t_0)$. Then the stochastic model equations are inte-

grated forward in time to obtain $\mathbf{U}^*(t)$ and $\mathbf{x}^*(t)$. The expected particle number density (at any $\mathbf{x}, t$) is then proportional to the mean contaminant concentration.

In Lagrangian PDF methods, the stochastic models are used to determine both Lagrangian and Eulerian pdfs. This is achieved through the fundamental relation:

$$f(\mathbf{V};\mathbf{x},t) = \iint f(\mathbf{V}_0;\mathbf{x}_0,t_0) f_{\mathrm{L}}(\mathbf{V},\mathbf{x};t|\mathbf{V}_0,\mathbf{x}_0)\, d\mathbf{V}_0\, d\mathbf{x}_0, \tag{19}$$

where integration is over all velocities and over the entire flow domain at t_0. (A derivation of this equation is given by Pope 1985.) Thus the Lagrangian pdf f_{L} is the *transition density* for the turbulent flow: It determines the transition of the Eulerian pdf from time t_0 to time t.

Since f_{L} determines f, it also determines simple Eulerian means, such as the mean velocity $\langle \mathbf{U}(\mathbf{x},t)\rangle$ and the Reynolds stresses $\langle u_i u_j\rangle$ (where $\mathbf{u} = \mathbf{U} - \langle \mathbf{U}\rangle$). Such means can therefore be used as coefficients in the stochastic Lagrangian models.

It is almost inevitable that computationally viable stochastic models are Markov processes. That is, with $t_{k-1} < t_k < t_{k+1}$, the joint pdf of $\mathbf{U}^*(t_{k+1})$ and $\mathbf{x}^*(t_{k+1})$ is completely determined by $\mathbf{U}^*(t_k)$, $\mathbf{x}^*(t_k)$ and the Eulerian pdf $f(\mathbf{V};\mathbf{x},t_k)$, independent of the particle properties at earlier times t_{k-1}. It then follows that (the model equivalent of) the M-time Lagrangian pdf (Equation 15) is given by the product of the M transition densities

$$f^*_{\mathrm{LM}}(\mathbf{V}_M,\mathbf{x}_M;t_M;\mathbf{V}_{M-1},\mathbf{x}_{M-1};t_{M-1};\ldots;\mathbf{V}_1,\mathbf{x}_1;t_1|\mathbf{V}_0,\mathbf{x}_0) = \prod_{k=1}^{M} f^*_{\mathrm{L}}(\mathbf{V}_k,\mathbf{x}_k;t_k|\mathbf{V}_{k-1},\mathbf{x}_{k-1}). \tag{20}$$

Thus for Markov models it is sufficient to consider the transition density f^*_{L} since this contains the same information as the M-time Lagrangian pdf.

Lagrangian PDF methods are implemented numerically as Monte Carlo/particle methods. In contrast to implementations for dispersion studies, the large number of particles are at all times uniformly distributed in the flow domain. This particle representation is described in more detail in Section 4. Calculations based on this approach are described by Haworth & Pope (1987), Anand et al (1989, 1993), Haworth & El Tahry (1991), Taing et al (1993), and Norris (1993), for example.

3. LANGEVIN EQUATION

The Langevin equation is the prototypical stochastic model. The basic mathematical and physical concepts are introduced here in a simple setting. More general and advanced models are described in Section 5.

We begin by considering stationary homogeneous isotropic turbulence, with zero mean velocity, turbulence intensity u', and Lagrangian integral time scale T. The subject of the Langevin equation, $U^*(t)$, is a model for one component of the fluid-particle velocity $U^+(t)$.

Written as a stochastic differential equation (sde), the Langevin equation is

$$dU^*(t) = -U^*(t)\,dt/T + (2u'^2/T)^{1/2}\,dW(t), \tag{21}$$

where $W(t)$ is a Wiener process. The reader unfamiliar with sdes, can appreciate the meaning of the Langevin equation through the finite-difference approximation

$$U^*(t+\Delta t) = U^*(t) - U^*(t)\Delta t/T + (2u'^2\Delta t/T)^{1/2}\xi, \tag{22}$$

where ξ is a standardized Gaussian random variable ($\langle\xi\rangle = 0$, $\langle\xi^2\rangle = 1$) which is independent of the corresponding random variable on all other time steps. Thus the increment in the Wiener process $dW(t)$ can be thought of as a Gaussian random variable with mean zero, and variance dt.

The basic mathematical properties of the Langevin equation are now described, and then their relationship to the physics of turbulence is discussed.

The Langevin equation (Equation 21 or 22) describes a Markov process $U^*(t)$ that is continuous in time (see Gardiner 1990, for a more precise statement). Hence, in the terminology of stochastic processes, $U^*(t)$ is a *diffusion process*. Although it is continuous, it is readily seen that $U^*(t)$ is not differentiable: Equation (22) shows that $[U^*(t+\Delta t) - U^*(t)]/\Delta t$ varies as $\Delta t^{-1/2}$, and hence does not converge as Δt tends to zero.

For simplicity we consider the initial condition at time t_0 that $U^*(t_0)$ is a Gaussian random variable with zero mean and variance u'^2. Then, for $t > t_0$, $U^*(t)$ is the stationary random process known as the *Ornstein-Uhlenbeck (OU) process*, a sample of which is shown on Figure 1. The OU process is a stationary, Gaussian, Markov process, and hence is completely characterized by its mean ($\langle U^*(t)\rangle = 0$), its variance ($\langle U^*(t)^2\rangle = u'^2$), and its autocorrelation function, which is

$$\rho^*(s) \equiv \langle U^*(t+s)U^*(t)\rangle/u'^2 = e^{-|s|/T}, \tag{23}$$

(see e.g. Gardiner 1990). Notice that these results confirm the consistency of the specification of the coefficients in the Langevin equation: The rms fluid-particle velocity is u', and the Lagrangian integral time scale is

$$T = \int_0^\infty \rho^*(s)\, ds. \tag{24}$$

To what extent does $U^*(t)$ model the fluid particle velocity $U^+(t)$? The first and obvious limitation is that $U^+(t)$ is differentiable, whereas $U^*(t)$ is not. Hence the model is qualitatively incorrect if $U^*(t)$ is examined on an infinitesimal time scale.

But consider high Reynolds number turbulence in which there is a large separation between the integral time scale T and the Kolmogorov time scale τ_η; and let us examine $U^+(t)$ on inertial-range time scales s, $T \gg s \gg \tau_\eta$. This is best done through the Lagrangian structure function (see e.g. Monin & Yaglom 1975)

$$D_L(s) \equiv \langle [U^+(t+s) - U^+(t)]^2 \rangle. \tag{25}$$

The Kolmogorov hypotheses (both original 1941 and refined 1962) predict (in the inertial range)

$$D_L(s) = C_0 \langle \varepsilon \rangle s, \tag{26}$$

where C_0 is a universal constant, and $\langle \varepsilon \rangle$ is the mean dissipation rate. And the Langevin equation yields [for the structure function based on $U^*(t)$]:

$$D_L^*(s) = 2u'^2 s/T, \quad \text{for} \quad s/T \ll 1, \tag{27}$$

as is evident from Equation (22). Thus the Langevin equation is consistent with the Kolmogorov hypotheses in yielding a linear dependence of D_L on s in the inertial range. (Equation 27 corresponds to an ω^{-2} frequency spectrum (at high frequency), which in turn corresponds to white-noise acceleration.)

By comparing the coefficients in Equations (26) and (27) we obtain the relation

$$T^{-1} = C_0 \langle \varepsilon \rangle / (2u'^2) = \tfrac{3}{4} C_0 \langle \varepsilon \rangle / k, \tag{28}$$

where k is the turbulent kinetic energy; and the Langevin equation (Equation 21) can be rewritten in the alternative form:

$$dU^*(t) = -\frac{3}{4} C_0 \frac{\langle \varepsilon \rangle}{k} U^*(t)\, dt + (C_0 \langle \varepsilon \rangle)^{1/2}\, dW(t). \tag{29}$$

To date, Lagrangian statistics in high-Reynolds number flows have proven inaccessible both to experiment and to direct numerical simulation. Consequently, a direct test of Equation (26) has not been possible. However at low or moderate Reynolds number, both techniques have been

used to measure the Lagrangian autocorrelation function $\rho(s)$. Figure 2 shows the results compared to the exponential (Equation 23) arising from the Langevin equation. At very small times s/T, the behavior is qualitatively different because $U^*(t)$ is not differentiable—correspondingly, $\rho^*(s)$ has negative slope at the origin. But for larger times, the exponential form provides a very reasonable approximation to the observed autocorrelations.

Measurements on turbulent dispersion provide an indirect test of the Langevin equation. For particles originating from the origin at time $t = 0$, their subsequent position is

$$x^*(t) = \int_0^t U^*(t')\,dt'. \tag{30}$$

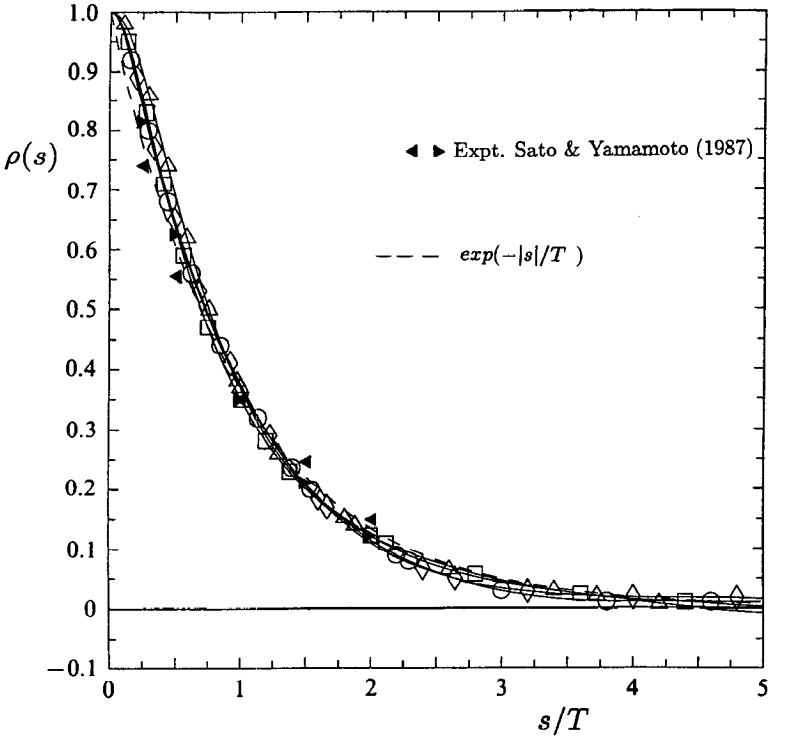

Figure 2 Lagrangian velocity autocorrelation function in isotropic turbulence: open symbols and lines from DNS of Yeung & Pope (1989); full symbols from experiments of Sato & Yamamoto (1987); dashed line exponential, Equation 23. (From Yeung & Pope 1989.)

This (according to the Langevin equation) is a Gaussian process, with zero mean, and variance

$$\langle x^*(t)^2 \rangle = 2u'^2 T[t - T(1 - e^{-t/T})], \tag{31}$$

which exhibits the correct short-time limit [$\langle x^*(t)^2 \rangle \approx (u't)^2$] and long-time limit [$\langle x^*(t)^2 \rangle \approx 2u'^2 Tt$] given by Taylor's (1921) theory.

The Langevin equation has been applied to dispersion behind a line source in grid turbulence by Anand & Pope (1985) with modifications to account for the decay of the turbulence and the first-order effects of molecular diffusion. The result shown on Figure 3 is in excellent agreement with the data.

Several refinements and extensions to the Langevin equation are described in Section 5, where further comparisons with DNS data are made.

We now describe the most rudimentary extension of the Langevin equation to inhomogeneous flows. The equation is a model for the evolution of all three components of velocity $\mathbf{U}^*(t)$ of a fluid particle with position $\mathbf{x}^*(t)$.

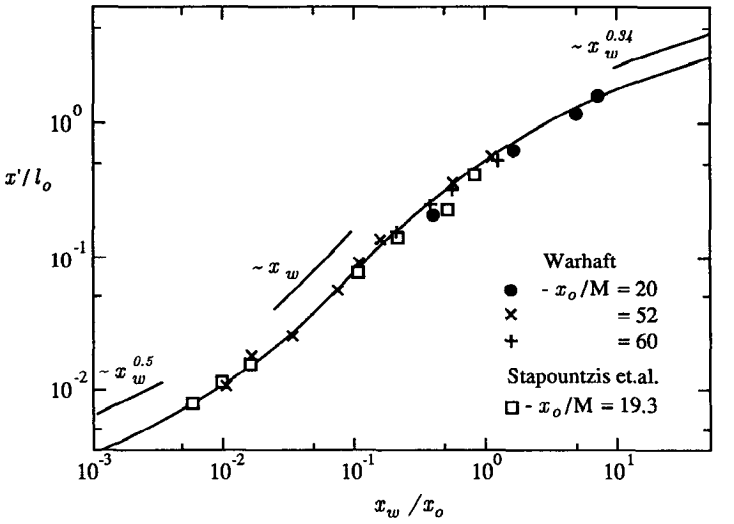

Figure 3 Turbulent dispersion behind a line source in grid turbulence. The rms dispersion $x' = \langle x^{*2} \rangle^{1/2}$ is normalized by the integral scale at the source l_o; the distance downstream of the source x_w is normalized by the distance from the grid to the source x_o. Experimental data of Warhaft (1984) and of Stapountzis et al (1986). Solid line is the calculation of Anand & Pope (1985) based on the Langevin equation.

There are three modifications to Equation (29)—all to the drift term. First, the velocity increment due to the mean pressure gradient $-dt\nabla\langle p\rangle$ is added. Second, the fluid particle velocity relaxes to the local Eulerian mean $\langle\mathbf{U}(\mathbf{x}^*[t], t)\rangle$ (rather than to zero). And, third, the coefficient of the drift term is altered. The result is

$$d\mathbf{U}^*(t) = -\nabla\langle p\rangle\, dt - \left(\frac{1}{2}+\frac{3}{4}C_0\right)\frac{\langle\varepsilon\rangle}{k}(\mathbf{U}^*(t)-\langle\mathbf{U}\rangle)\, dt + (C_0\langle\varepsilon\rangle)^{1/2}\, d\mathbf{W}(t). \quad (32)$$

In this (and subsequent) equations, it is understood that mean quantities (i.e. $\nabla\langle p\rangle$, $\langle\varepsilon\rangle$, k and $\langle\mathbf{U}\rangle$) are evaluated at the fluid-particle position $\mathbf{x}^*(t)$. The vector-valued Wiener process $\mathbf{W}(t)$ is simply composed of three independent components $W_1(t)$, $W_2(t)$, and $W_3(t)$. The increment $d\mathbf{W}$ has zero mean and covariance

$$\langle dW_i\, dW_j\rangle = dt\,\delta_{ij}. \quad (33)$$

[As discussed at greater length in Section 5.1, the coefficient $(\frac{1}{2}+\frac{3}{4}C_0)$ in Equation (32) (compared to $\frac{3}{4}C_0$ in Equation 29), correctly causes the turbulent kinetic energy to be dissipated at the rate $\langle\varepsilon\rangle$. The omission of the $\frac{1}{2}$ in Equation (29) is because that equation pertains to the hypothetical case of stationary (i.e. non-decaying) isotropic turbulence.]

A stochastic model for fluid-particle properties implies a modeled evolution equation for the corresponding Lagrangian joint pdf. In the present context, $f_{\mathrm{L}}^*(\mathbf{V}, \mathbf{x}, t|\mathbf{V}_0, \mathbf{x}_0)$ is the joint pdf of $\mathbf{U}^*(t)$ and $\mathbf{x}^*(t)$, with the initial conditions $\mathbf{U}^*(t_0) = \mathbf{V}_0$, $\mathbf{x}^*(t_0) = \mathbf{x}_0$. Then with $\mathbf{U}^*(t)$ evolving by the extended Langevin equation (Equation 32), and with $\mathbf{x}^*(t)$ evolving by Equation (17), f_{L}^* evolves according to the *Fokker-Planck equation*

$$\frac{\partial}{\partial t}f_{\mathrm{L}}^* = -V_i\frac{\partial f_{\mathrm{L}}^*}{\partial x_i} + \frac{\partial\langle p\rangle}{\partial x_i}\frac{\partial f_{\mathrm{L}}^*}{\partial V_i} + \left(\frac{1}{2}+\frac{3}{4}C_0\right)\frac{\langle\varepsilon\rangle}{k}\frac{\partial}{\partial V_i}[f_{\mathrm{L}}^*(V_i-\langle U_i\rangle)] + \frac{1}{2}C_0\langle\varepsilon\rangle\frac{\partial^2 f_{\mathrm{L}}^*}{\partial V_i\partial V_i}, \quad (34)$$

(see Gardiner 1990, Risken 1989), with the initial condition

$$f_{\mathrm{L}}^*(\mathbf{V}, \mathbf{x}, t_0|\mathbf{V}_0, \mathbf{x}_0) = \delta(\mathbf{V}-\mathbf{V}_0)\delta(\mathbf{x}-\mathbf{x}_0). \quad (35)$$

The Eulerian joint pdf of velocity $f(\mathbf{V}; \mathbf{x}, t)$ is related to its Lagrangian counterpart by Equation (19). Hence the above evolution equation for f_{L}^* implies a corresponding evolution equation for the modeled Eulerian pdf $f^*(\mathbf{V}; \mathbf{x}, t)$. Indeed, since the differential operators in the Fokker-Planck

equation are independent of t_0, $\mathbf{x}_0$, and $\mathbf{V}_0$, it follows immediately from Equation (19) that the Eulerian pdf $f^*(\mathbf{V}; \mathbf{x}, t)$ also evolves according to Equation (34).

The Eulerian pdf equation (i.e. Equation 34 written for f^*), together with a modeled equation for $\langle \varepsilon \rangle$, form a complete set of turbulence-model equations. They are complete in the sense that all the coefficients in Equation (34) are known in terms of f^* and $\langle \varepsilon \rangle$. The mean velocity $\langle \mathbf{U} \rangle$ and the kinetic energy k are determined as first and second moments of f^*, while the mean pressure field $\langle p \rangle$ is determined as the solution of a Poisson equation. The source in the Poisson equation involves $\langle \mathbf{U} \rangle$ and $\langle u_i u_j \rangle$ which are known in terms of f^*.

In Section 5.3 coupled stochastic models for $\mathbf{U}^*(t)$ and $\omega^*(t) \equiv \varepsilon^*(t)/k$ are described, which lead to an evolution equation for the joint pdf of $\mathbf{U}$ and ω. This single equation provides a complete model: All of the coefficients are known in terms of the pdf itself.

The above development illustrates the different use of the Langevin equation in turbulent dispersion and in PDF methods. In the former, the turbulent flow field is assumed known, and so the coefficients in the Langevin equation are specified; and the equation is used (at most) to deduce the Lagrangian pdf. In PDF methods, the Langevin equation is used to determine the Eulerian pdf, from which the coefficients are deduced.

4. PARTICLE REPRESENTATION

Central to Lagrangian PDF methods is the idea that a turbulent flow can be represented by an ensemble of N fluid particles, with positions and velocities $\mathbf{x}^{(n)}(t)$, $\mathbf{U}^{(n)}(t)$, $n = 1, 2, \ldots, N$. The purpose of this section is to describe this particle representation, and to make precise the connection between particle properties and statistics of the flow.

4.1 *Basic Representation*

We begin by considering a single component of velocity U at a particular point and time. Thus U is a random variable, with pdf $f(V)$, which we consider to be known.

For a given ensemble size $N (N \geq 1)$, the particle velocities $\{U^{(n)}\}$ are specified to be independent random samples, each with pdf $f(V)$. It is conceptually useful (and legitimate) to think of $U^{(n)}$ as the value of U on the n-th (independent) realization of the flow. Note that the particle velocities are independent and identically distributed, and hence the numbering of the particles is irrelevant.

A fundamental question, to which we provide three answers, is: In what

sense does the ensemble $\{U^{(n)}\}$ "represent" the underlying distribution $f(V)$?

The first answer is in terms of the discrete pdf $f_N(V)$, defined by

$$f_N(V) \equiv \frac{1}{N} \sum_{n=1}^{N} \delta(U^{(n)} - V). \tag{36}$$

It is readily shown (see, e.g. Pope 1985) that the *expected* discrete pdf equals $f(V)$ for *any* $N \geq 1$:

$$\langle f_N(V) \rangle = f(V). \tag{37}$$

In the analysis of PDF methods, this relation allows properties of the pdf [i.e. $f(V)$] to be deduced from the properties of a single particle ($U^{(1)}$, say).

The second answer involves ensemble averages. In numerical implementations of PDF methods it is necessary to *estimate* means such as $\langle U \rangle$ and $\langle U^2 \rangle$ from the ensemble $\{U^{(n)}\}$. Let $Q(U)$ be some function of the velocity U, then we have

$$\langle Q(U) \rangle = \int_{-\infty}^{\infty} f(V) Q(V)\, dV. \tag{38}$$

For example, the choices of V and V^2 for $Q(V)$ lead to $\langle U \rangle$ and $\langle U^2 \rangle$. The mean $\langle Q \rangle$ can be estimated from the ensemble simply as the ensemble average

$$\langle Q(U) \rangle_N \equiv \frac{1}{N} \sum_{n=1}^{N} Q(U^{(n)}) = \int_{-\infty}^{\infty} f_N(V) Q(V)\, dV. \tag{39}$$

Then (since $\{U^{(n)}\}$ are independent and identically distributed) a basic result from statistics is that $\langle Q \rangle_N$ is an unbiased estimator of $\langle Q \rangle$:

$$\langle \langle Q \rangle_N \rangle = \langle Q \rangle. \tag{40}$$

Further, if the variance of $Q(U)$ is finite, it follows from the central limit theorem that for large N the rms statistical error in $\langle Q \rangle_N$ tends to zero as $N^{-1/2}$.

Hence the second sense in which the ensemble $\{U^{(n)}\}$ "represents" the pdf $f(V)$ is that, for all functions Q [for which $Q(U)$ has finite mean and variance], the ensemble average $\langle Q \rangle_N$ converges in mean square to $\langle Q \rangle$. This is written

$$\lim_{N \to \infty} \langle Q \rangle_N = \langle Q \rangle. \tag{41}$$

[An additional convergence result is provided by the Glivenko-Cantelli theorem (e.g. Billingsley 1986): As N tends to infinity, the difference

between the cdf $F(V)$ and the *empirical cdf* $F_n(V)$—i.e. the definite integral of $f_N(V)$—converges to zero with probability one.]

For almost all purposes, the two answers provided above are sufficient: Equation (37) is used in the analysis of PDF methods, while Equation (41) is used in numerical implementations. However, neither of these relations (nor the Glivenko-Cantelli theorem) provides an estimate of the pdf $f(V)$ in terms of $\{U^{(n)}\}$ that converges in mean square as N tends to infinity. The third answer, then, is that the techniques of *density estimation* can be used for this purpose (see e.g. Tapia & Thompson 1978, Silverman 1986). These are not reviewed here, since they have not played an important role in PDF methods. This is because in the implementation of PDF methods, an *explicit* representation of the pdf is not required.

The above considerations apply to any random variable U. Consider now $U^{(n)}(t)$ to be a model for the velocity of a fluid particle, obtained as the solution to a stochastic model equation—the Langevin equation, for example. At the initial time t_0, the values of $\{U^{(n)}(t_0)\}$ are sampled from the specified initial pdf $f(V; t_0)$.

The representations described above are readily extended. The one-time discrete pdf [representing $f(V; t)$] is

$$f_N(V; t) = \frac{1}{N} \sum_{n=1}^{N} \delta[U^{(n)}(t) - V], \tag{42}$$

while the discrete Lagrangian pdf is

$$f_{LN}(V; t | V_0) = \frac{1}{N} \sum_{n=1}^{N} \{\delta[U^{(n)}(t) - V] | U^{(n)}(t_0) = V_0\}. \tag{43}$$

Multi-time Lagrangian statistics can be estimated as ensemble averages: for example,

$$\langle Q(U(t_1), U(t_2))\rangle_N \equiv \frac{1}{N} \sum_{n=1}^{N} Q[U^{(n)}(t_1), U^{(n)}(t_2)]. \tag{44}$$

4.2 *Inhomogeneous Flows*

The extension of this particle representation to inhomogeneous flows requires some new ingredients, and it leads to some subtle consistency conditions.

Throughout, for simplicity, we are restricting our attention to constant-density flows in a material volume. Hence the volume V of the flow domain D, and the mass of fluid within it, do not change with time.

At a given time t, an ensemble of N particles is constructed as follows to represent the joint pdf of velocity $f(\mathbf{V}; \mathbf{x}, t)$. The particle positions $\mathbf{x}^{(n)}(t)$

are mutually independent, random, uniformly-distributed in D. [Hence the pdf of each $\mathbf{x}^{(n)}(t)$ is 1/V.] Then the particle velocity $\mathbf{U}^{(n)}(t)$ is random, with pdf $f[\mathbf{V}; \mathbf{x}^{(n)}(t), t]$. In terms of these properties, the discrete pdf is defined by

$$f_N(\mathbf{V}; \mathbf{x}, t) \equiv \frac{\mathrm{V}}{N} \sum_{i=1}^{N} \delta[\mathbf{x}^{(n)}(t) - \mathbf{x}] \delta[\mathbf{U}^{(n)}(t) - \mathbf{V}]. \tag{45}$$

The specification of $\mathbf{x}^{(n)}(t)$ (and also the constant in Equation 45) is determined by a consistency condition. We require the expectation of f_N to equal f; where f satisfies the normalization condition that its integral over all $\mathbf{V}$ is unity. Hence from Equation (45) we obtain

$$1 = \int \langle f_N \rangle \, d\mathbf{V} = \mathrm{V} \langle \delta[\mathbf{x}^{(n)}(t) - \mathbf{x}] \rangle, \tag{46}$$

for any n (since $\{\mathbf{x}^{(n)}\}$ are independent and identically distributed). This condition is satisfied if, and only if, $\mathbf{x}^{(n)}(t)$ is uniformly distributed.

If this consistency condition is satisfied at an initial time t_0, will it remain satisfied as the particle properties evolve in time? The answer (established by Pope 1985, 1987) is yes, provided the mean continuity equation is satisfied. This in turn requires that the mean pressure gradient [affecting the evolution of $\mathbf{U}^{(n)}(t)$, Equation 32] satisfies the appropriate Poisson equation.

Both of these results are reflected in the Eulerian pdf equation [e.g. Equation 34 written for $f(\mathbf{V}; \mathbf{x}, t)$]. When this equation is integrated over all $\mathbf{V}$, all the terms on the right-hand side vanish, expect the first which is $-\nabla \cdot \langle \mathbf{U} \rangle$. If this is nonzero—in violation of the continuity equation—then the normalization condition on f is also violated. An evolution equation for $\nabla \cdot \langle \mathbf{U} \rangle$ is obtained from Equation (34) by multiplying by V_j, integrating over all $\mathbf{V}$, and then differentiating with respect to x_j. Equating the time rate of change of $\nabla \cdot \langle \mathbf{U} \rangle$ to zero, yields a Poisson equation for $\langle p \rangle$.

With $Q(\mathbf{V})$ being a function of the velocity, we now consider the estimation of the mean $\langle Q[\mathbf{U}(\mathbf{x}, t)] \rangle$ from the ensemble of particles. This is an important issue because Eulerian means such as $\langle \mathbf{U} \rangle$ and $\langle u_i u_j \rangle$ must be estimated from the particle properties in order to determine the coefficients in the modeled particle evolution equations, e.g. Equation (32).

Since (with probability one) there are no particles located at $\mathbf{x}$, it is unavoidable that an estimate of $\langle Q[\mathbf{U}(\mathbf{x}, t)] \rangle$ must involve particles in the vicinity of $\mathbf{x}$. We describe now the *kernel estimator* (see e.g. Eubank 1988, Härdle 1990), which is useful both conceptually and in practice (although a literal implementation is not efficient). It is assumed that $Q[\mathbf{U}(\mathbf{x}, t)]$

has finite mean and variance, and that the mean is twice continuously differentiable with respect to $\mathbf{x}$.

For simplicity we consider points $\mathbf{x}$ that are remote from the boundary of the domain; and for definiteness we take the kernel to be a Gaussian of specified width h. In D dimensions this is

$$K(\mathbf{r}, h) = (\sqrt{2\pi}h)^{-D} \exp(-\tfrac{1}{2}r^2/h^2), \tag{47}$$

(where $r = |\mathbf{r}|$). Then a kernel estimator of $\langle Q[\mathbf{U}(\mathbf{x}, t)]\rangle$ is

$$\langle Q[\mathbf{U}(\mathbf{x}, t)]\rangle_{N,h} \equiv \frac{\mathsf{V}}{N} \sum_{n=1}^{N} K[\mathbf{x} - \mathbf{x}^{(n)}(t), h] Q[\mathbf{U}^{(n)}(t)]. \tag{48}$$

For small h, the bias in this estimate is

$$\langle\langle Q\rangle_{N,h}\rangle - \langle Q\rangle = \tfrac{1}{2}h^2\nabla^2\langle Q\rangle + \mathsf{O}(h^4). \tag{49}$$

Hence, as h tends to zero, $K(\mathbf{r}, h)$ tends to $\delta(\mathbf{r})$ and $\langle\langle Q\rangle_{N,h}\rangle$ converges to $\langle Q\rangle$.

But as h becomes smaller, fewer particles have significant values of $K[\mathbf{x} - \mathbf{x}^{(n)}(t), h]$, and so the statistical error rises: The variance of $\langle Q\rangle_{N,h}$ varies as

$$\mathsf{V}/(Nh^D) = (L/h)^D/N, \tag{50}$$

where $L \equiv \mathsf{V}^{1/D}$ is a characteristic length of the domain. It is readily shown that, for large N, it is optimal for h/L to vary as $N^{-1/(4+D)}$. For then, the sum of the bias and the rms statistical error is minimized, each varying as $N^{-2/(4+D)}$. Thus, for such a choice of h we have

$$\lim_{N\to\infty} \langle Q\rangle_{N,h} = \langle Q\rangle. \tag{51}$$

These results have two major significances. First, Equation (51) shows the convergence of the particle representation. Second, it is likely that in a numerical implementation the error decreases with increasing N no faster than $N^{-2/(4+D)}$.

Although it is seldom done in practice, it is in principle possible to use the above ideas to extract multi-time Lagrangian statistics. It is important to realize, however, that (at a fixed time) the particle representation contains no two-point information. Recall that different particles can be viewed as being sampled from different, independent realizations of the flow.

5. STOCHASTIC LAGRANGIAN MODELS

5.1 *Generalized Langevin Model*

The Langevin equation for inhomogeneous flows described in Section 3 (Equation 32) is referred to as the *Simplified Langevin Model* (SLM). It is the simplest possible extension of the basic Langevin model (Equation 29) that is consistent with momentum and energy conservation.

The *Generalized Langevin Model* (GLM)—proposed by Pope (1983a) and developed and demonstrated by Haworth & Pope (1986, 1987)—overcomes some of the qualitative and quantitative defects of the SLM. For the increment in the fluid-particle velocity $\mathbf{U}^*(t)$, the GLM is

$$dU_i^* = -\frac{\partial \langle p \rangle}{\partial x_i}\,dt + \mathcal{G}_{ij}(U_j^* - \langle U_j \rangle)\,dt + (C_0\langle \varepsilon \rangle)^{1/2}\,dW_i, \tag{52}$$

where the drift coefficient tensor $\mathcal{G}_{ij}$ is a modeled function of the local mean velocity gradients $\partial\langle U_i\rangle/\partial x_j$, Reynolds stresses $\langle u_i u_j\rangle$, and dissipation $\langle\varepsilon\rangle$. It may be immediately observed that the SLM corresponds to the simple specification

$$\mathcal{G}_{ij} = \mathcal{G}_{ij}^0 \equiv -\left(\frac{1}{2} + \frac{3}{4}C_0\right)\frac{\langle \varepsilon \rangle}{k}\,\delta_{ij}. \tag{53}$$

Hence the GLM is distinguished by a more elaborate specification of $\mathcal{G}_{ij}$.

The first term in Equation (52) is uniquely determined by the mean momentum equations (at high Reynolds number, when the viscous term is negligible). The final term in Equation (52) (the diffusion term) has the same form as in homogeneous isotropic turbulence. This is justified (at high Reynolds number) by the Kolmogorov (1941) hypotheses: The term pertains to small time-scale (high frequency) processes that are hypothesized to be locally isotropic and characterized by $\langle\varepsilon\rangle$. (Implications of the Kolmogorov 1962 hypotheses are discussed in Section 5.3, and Reynolds-number effects in 5.4.)

In the construction of the drift term (involving $\mathcal{G}_{ij}$), the principal assumption made is that the term is linear in $\mathbf{U}^*$. For homogeneous turbulence, the assumption is fully justified, since this linearity is necessary and sufficient (Arnold 1974) for the joint pdf of velocity to be joint normal, in accord with experimental observations (e.g. Tavoularis & Corrsin 1981).

The observed joint normality of the one-point velocity pdf in homogeneous turbulence leads to several important results. For this case, the joint pdf is fully determined by the (known) mean velocity, and by the covariance matrix, namely the Reynolds stresses; and, according to the GLM (Equation 52), the Reynolds stresses evolve by

$$\frac{d}{dt}\langle u_k u_l\rangle = \mathscr{P}_{kl} + \mathscr{G}_{ki}\langle u_i u_l\rangle + \mathscr{G}_{li}\langle u_i u_k\rangle + C_0\langle\varepsilon\rangle\delta_{kl}, \tag{54}$$

where $\mathscr{P}_{kl}$ is the production tensor:

$$\mathscr{P}_{kl} \equiv -\langle u_i u_k\rangle \frac{\partial\langle U_l\rangle}{\partial x_i} - \langle u_i u_l\rangle \frac{\partial\langle U_k\rangle}{\partial x_i}. \tag{55}$$

Thus for any choice of $\mathscr{G}_{ij}$ there is a corresponding modeled Reynolds-stress equation, which (as shown by Pope 1985) is realizable. The known behavior of the Reynolds stress equation in certain limits (e.g. rapid distortion, or two-component turbulence) can then be invoked to impose constraints on $\mathscr{G}_{ij}$.

Using these constraints and experimental data on homogeneous turbulence, Haworth & Pope (1986) determined a specific form of $\mathscr{G}_{ij}$ that accurately describes the evolution of the Reynolds stresses (and hence the velocity joint pdf) in these flows. As an example, Figure 4 shows the evolution of the anisotropy tensor

$$b_{ij} \equiv \langle u_i u_j\rangle/\langle u_i u_l\rangle - \tfrac{1}{3}\delta_{ij}, \tag{56}$$

for the plane strain experiment of Gence & Mathieu (1979).

As is customary in turbulence modeling, with simplicity as the main justification, the same model is used in inhomogeneous flows. Haworth &

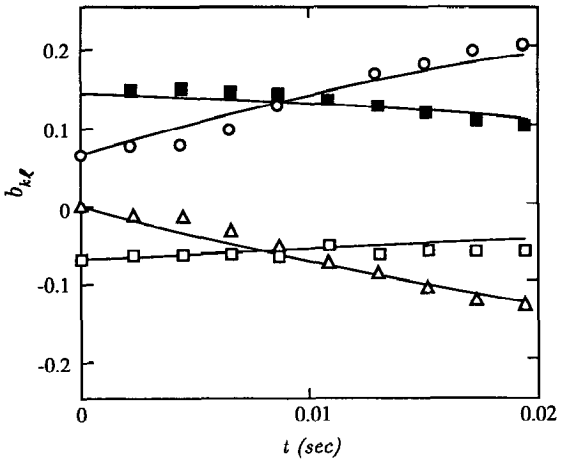

Figure 4 Reynolds stress anisotropies $b_{kl} \equiv \langle u_k u_l\rangle/\langle u_i u_i\rangle - \frac{1}{3}\delta_{kl}$ against time for transverse plane strain of homogeneous turbulence. Symbols: experimental data of Gence & Mathieu (1979) □ b_{11}, △ b_{22}, ○ b_{33}, ■ b_{23}. Lines: GLM calculations. (From Haworth & Pope 1986.)

Pope (1987) describe the successful application of the GLM to a range of free shear flows.

Finally, we observe that there is a Reynolds-stress equation corresponding to the SLM. Specifically, for homogeneous turbulence, Equations (52) and (53) lead to:

$$\frac{d}{dt}\langle u_k u_l\rangle = \mathscr{P}_{kl} - (2+3C_0)\langle\varepsilon\rangle b_{kl} - \tfrac{2}{3}\langle\varepsilon\rangle\delta_{kl}, \tag{57}$$

which is Rotta's (1951) model. Thus, in Reynolds-stress-closure terminology, the GLM is superior to the SLM in allowing for a nonlinear return-to-isotropy, and for incorporating "rapid pressure" effects. Recently Pope (1993) considered in detail the relationship between the GLM and Reynolds-stress models, and thereby deduced specifications corresponding to the isotropization of the production model (IPM, Naot et al 1970) and to the SSG model (Speziale et al 1991).

5.2 *Stochastic Model for Frequency*

The Generalized Langevin Model, just described, leads to a modeled transport equation for the velocity joint pdf $f(\mathbf{V}; \mathbf{x}, t)$. This equation does not provide a complete model, because the mean dissipation rate $\langle\varepsilon\rangle$ (or equivalent information) must be supplied separately—from a modeled transport equation for $\langle\varepsilon\rangle$, for example. This shortcoming motivated the development of a complete closure based on the joint pdf of velocity and dissipation (Pope & Chen 1990), which required the development of a stochastic model for dissipation.

In fact, rather than the instantaneous dissipation rate $\varepsilon(\mathbf{x}, t)$ the model developed by Pope & Chen (1990) is based on the *turbulence frequency* defined by

$$\omega(\mathbf{x}, t) \equiv \varepsilon(\mathbf{x}, t)/k(\mathbf{x}, t). \tag{58}$$

It should be noted that this is a mixed quantity in that $\varepsilon(\mathbf{x}, t)$ is random whereas $k(\mathbf{x}, t)$ is not. Thus the probability distribution of ω is the same as that of ε, to within a scaling. The mean frequency $\langle\omega\rangle$ has been used previously as a turbulence-model variable by, for example, Kolmogorov (1942) and Wilcox (1988).

For homogeneous turbulence, Pope & Chen (1990) developed a stochastic model $\omega^*(t)$ for the turbulent frequency following a fluid particle, $\omega^+(t)$. Their model is constructed by reference to the Lagrangian statistics of dissipation extracted from direct numerical simulations by Yeung & Pope (1989).

The simulations show that (to a very good approximation) the one-

point one-time distribution of ε is log-normal. That is, for fixed t, the random variable

$$\chi^+(t) \equiv \ln[\varepsilon^+(t)/\langle\varepsilon\rangle] = \ln[\omega^+(t)/\langle\omega\rangle], \tag{59}$$

is Gaussian, with variance denoted by σ^2. Further, except near the origin, the autocorrelation function of $\chi^+(t)$, $\rho_\chi(s)$, is well approximated by the exponential

$$\rho_x(s) = e^{-|s|T_\chi}. \tag{60}$$

where T_χ is the corresponding integral time scale. The simulations support the approximation

$$T_\chi^{-1} = C_\chi\langle\omega\rangle, \tag{61}$$

with C_χ being a constant.

Given that $\chi^+(t)$ has a Gaussian pdf and an exponential autocorrelation, it is obvious to model it as an OU process. The appropriate stochastic differential equation is

$$d\chi^*(t) = -[\chi^*(t) - \langle\chi^*(t)\rangle]\,dt/T_\chi + (2\sigma^2/T_\chi)^{1/2}\,dW, \tag{62}$$

(cf Equation 21).

The modeled frequency is related to χ^* by

$$\omega^*(t) = \langle\omega(t)\rangle e^{\chi^*(t)}, \tag{63}$$

(cf Equation 59). Consequently, in order to obtain a model equation for ω^*, it is necessary also to model the evolution of $\langle\omega\rangle$. With the nondimensional rate of change S_ω defined by

$$\frac{d\langle\omega\rangle}{dt} = -\langle\omega\rangle^2 S_\omega, \tag{64}$$

the standard model equation for $\langle\varepsilon\rangle$ (Launder & Spalding 1972) implies

$$S_\omega = (C_{\varepsilon 2} - 1) - (C_{\varepsilon 1} - 1)P/\langle\varepsilon\rangle, \tag{65}$$

where $C_{\varepsilon 1}$ and $C_{\varepsilon 2}$ are standard model constants, and P is the rate of production of turbulence kinetic energy.

The stochastic model for ω^* proposed by Pope & Chen (1990) is then obtained from Equations (62)–(64):

$$d\omega^* = -\omega^*\langle\omega\rangle\,dt\{S_\omega + C_\chi[\ln(\omega^*/\langle\omega\rangle) - \tfrac{1}{2}\sigma^2]\} + \omega^*(2C_\chi\langle\omega\rangle\sigma^2)^{1/2}\,dW. \tag{66}$$

The above development pertains to homogeneous turbulence. The extension of the model to inhomogeneous flows is considered by Pope (1991b).

The only significant modification required to Equation (66) is the addition of a term that (under appropriate circumstances) causes nonturbulent fluid (characterized by $\omega^* = 0$) to become turbulent ($\omega^* > 0$). As described in the next subsection, with this modification, the stochastic model for frequency is successful in describing the intermittent turbulent/nonturbulent regions of free shear flows.

5.3 *Refined Langevin Model*

The stochastic model for frequency $\omega^*(t)$ (Equation 66) can be combined with the Generalized Langevin Model (Equation 52) to provide a closed modeled joint pdf equation. However, if the frequency $\omega^*(t)$ following a fluid particle is known, it is possible to incorporate this information in a stochastic model for velocity so as to increase its physical realism. Such a refined Langevin model has been developed by Pope & Chen (1990) and Pope (1991b).

According to all of the Langevin equations described above, for a small time interval s ($s/T \ll 1$), the modeled Lagrangian velocity increment

$$\Delta_s \mathbf{U}^*(t) \equiv \mathbf{U}^*(t+s) - \mathbf{U}^*(t), \tag{67}$$

is an isotropic Gaussian random vector with covariance

$$\langle \Delta_s U_i^*(t) \Delta_s U_j^*(t) \rangle = C_0 \langle \varepsilon \rangle s \delta_{ij} + \mathrm{O}(s^2). \tag{68}$$

This covariance is consistent with the refined Kolmogorov (1962) hypotheses; but the Gaussianity of $\Delta_s \mathbf{U}^*(t)$ is clearly at odds with notions of internal intermittency. In the spirit of Kolmogorov's refined hypotheses, it is natural to model $\Delta_s \mathbf{U}^*(t)$ in terms of the particle dissipation $\varepsilon^*(t) = k\omega^*(t)$. This is simply achieved by replacing the diffusion coefficient $C_0\langle\varepsilon\rangle$ in the Langevin equation by $C_0\varepsilon^*$. Then, the *conditional* covariance of $\Delta_s \mathbf{U}(t)$ is

$$\langle \Delta_s U_i^*(t) \Delta_s U_j^*(t) | \varepsilon^*(t) = \hat{\varepsilon} \rangle = C_0 \hat{\varepsilon} s \delta_{ij} + \mathrm{O}(s^2), \tag{69}$$

while, correctly, the unconditional variance is again given by Equation (68).

Since the performance of the GLM is completely satisfactory for homogeneous turbulence, Pope & Chen (1990) developed the *Refined Langevin model* (RLM) to retain this behavior (while replacing $C_0\langle\varepsilon\rangle$ by $C_0\varepsilon^* = C_0 k\omega^*$ in the diffusion term). For homogeneous turbulence the model is

$$dU_i^* = -\frac{\partial \langle p \rangle}{\partial x_i} dt + \mathscr{L}_{ij}(U_j^* - \langle U_j \rangle)\, dt + (C_0 k \omega^*)^{1/2}\, dW_i, \tag{70}$$

where

$$\mathscr{L}_{ij} = \mathscr{G}_{ij} - \tfrac{3}{4}C_0(\omega^* - \langle\omega\rangle)\mathscr{B}_{ij}, \tag{71}$$

and the tensor $\mathscr{B}_{ij}$ is the inverse of $\langle u_i u_j\rangle/(\frac{2}{3}k)$. Notice that, compared to the GLM (Equation 52), the additional term in $\mathscr{B}_{ij}$ is needed to produce the correct Gaussian joint pdf of velocity (in homogeneous turbulence). Additional modifications for inhomogeneous flows are described by Pope (1991b).

The combination of the stochastic model for $\omega^*(t)$ (Equation 66) and the RLM for $\mathbf{U}^*(t)$ provides a closed modeled evolution equation for their joint pdf. This is the most advanced pdf model currently available. It has been applied to several different flows by Pope (1991b), Anand et al (1993), and Norris (1993). Calculations for a plane mixing layer are now briefly reported in order to illustrate several features of the model.

The calculations pertain to the statistically plane, two-dimensional, self-similar mixing layer formed between two uniform streams of different velocities. The dominant flow direction is x_1; the lateral direction is x_2; and the flow is statistically homogeneous in the spanwise direction x_3. The free-stream velocities are U_∞ (at $x_2 = \infty$) and $2U_\infty$ (at $x_2 = -\infty$), so that the velocity ratio is 2, and the velocity difference is $\Delta U = U_\infty$. At large axial distances the flow spreads linearly and is self-similar. Consequently, statistics of $\mathbf{U}(\mathbf{x}, t)/\Delta U$ depend only on x_2/x_1 [where $(x_1, x_2) = (0, 0)$ is the virtual origin of the mixing layer]. Lang (1985) provides experimental data on this flow. The calculations are performed by integrating the stochastic differential equations for the properties $(\mathbf{x}^{(n)}, \mathbf{U}^{(n)}, \omega^{(n)}; n = 1, 2, \ldots, N)$ of $N \approx 50{,}000$ particles. A comparison of the mean and rms velocities with experimental data shows good agreement (see Pope 1991b).

Figure 5 is a scatter plot of the axial velocity and lateral position. For this flow, with extremely high probability, there is no reverse flow (i.e. $U_1^{(n)}(t) > 0$ for all n and t). Hence the axial location $x_1^{(n)}(t)$ of each particle increases monotonically with time. Figure 5 is constructed by plotting the points $(U_1^{(n)}/\Delta U,\ x_2^{(n)}/x_1)$ for about one fifth of the particles (selected at random) as they pass a particular axial location x_1. (In view of self-similarity, the value of x_1 is immaterial.)

At large and small values of x_2^*/x_1, the points are dense at $U_1^*/\Delta U = 1$ and 2, respectively, and so appear as horizontal straight lines. These points correspond to fluid with the free-stream velocity. At the center of the layer (e.g. $x_2^*/x_1 = 0$), the points are broadly scattered in $U_1^*/\Delta U$, indicative of turbulent fluctuations with rms of order 0.2. Toward the edges of the layer, bimodal behavior is evident: with increasing distance from the layer, a band of points tends to the free-stream velocity, while other points exhibit fluctuations of order 0.1, but with decreasing probability. This reflects the turbulent/nonturbulent nature of these regions.

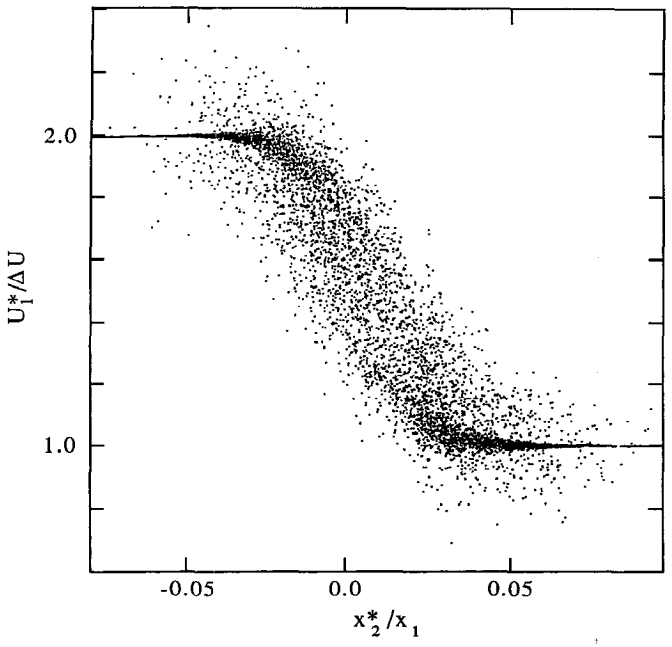

Figure 5 Scatter plot of axial velocity and lateral position from joint pdf calculations of the self-similar plane mixing layer (from Pope 1991b).

The intermittent nature of the edges of the mixing layer is yet more evident in Figure 6, which is a scatter plot of frequency and lateral position. The frequency is normalized by its maximum mean value $\langle\omega\rangle_{max}$ (at the axial location considered) and is shown on a logarithmic scale. At the edges of the layer the bimodal nature of ω^* is clear: There is a diffuse band of points centered around $\omega^* \sim 0.3\langle\omega\rangle_{max}$, with a second denser band with ω^* values two or three orders of magnitude less. These bands correspond to turbulent and nonturbulent fluid respectively.

For inhomogeneous flows, experimental data on Lagrangian quantities are essentially nonexistent. For this reason, there has been little impetus to extract Lagrangian statistics from pdf calculations. However, as an illustration of the type of information that is available in Lagrangian PDF methods, shown on Figure 7 are the fluid particle paths of five particles whose initial positions were selected at random near the center of the self-similar mixing layer. It may be observed that several of these trajectories traverse the layer monotonically, and that the trajectories are devoid of high wave number fluctuations. From this we conclude that the motion

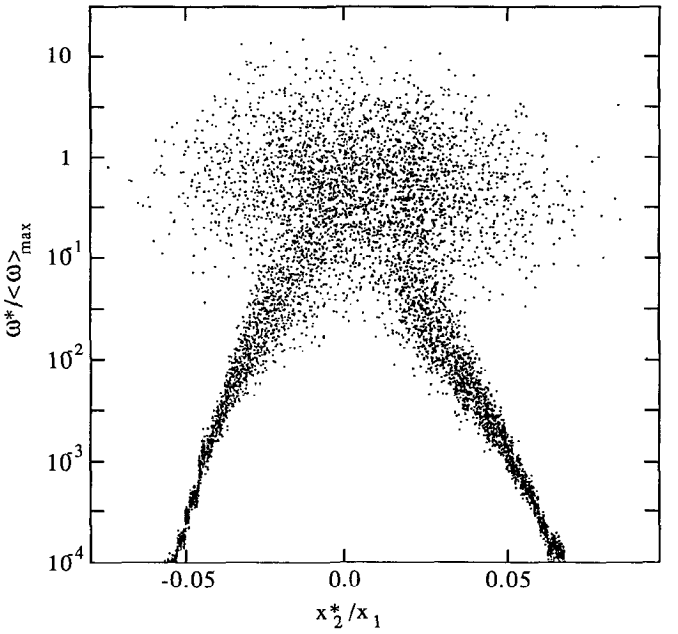

Figure 6 Scatter plot of turbulence frequency and lateral position from joint pdf calculations of the self-similar plane mixing layer (from Pope 1991b).

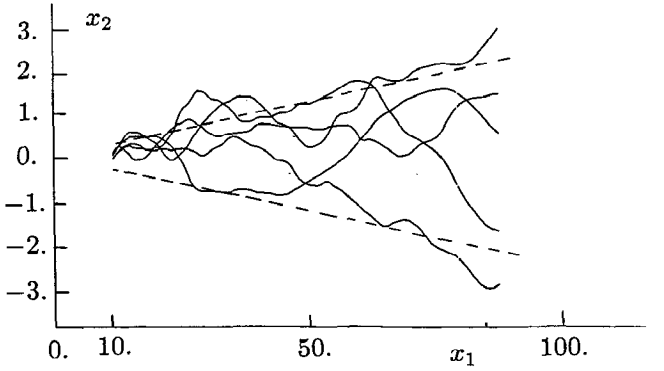

Figure 7 Fluid particle paths in the self-similar plane mixing layer according to stochastic models: x_1 and x_2 have arbitrary units. The dashed lines show the nominal edge of the layer, where the mean velocity differs from the free-stream velocity by 10% of the velocity difference. (From Pope 1991b.)

implied by the model is consistent with the large-scale coherent motions observed experimentally in mixing layers; and, conversely, it does not resemble the small-scale random motion analogous to molecular diffusion or Brownian motion.

5.4 *Stochastic Model for Acceleration*

When examined in detail, the basic Langevin model (described in Section 3) can be justified on physical grounds only in the limit of infinite Reynolds number Re. Sawford (1991) presents a stochastic model for the fluid particle acceleration which is extremely valuable and successful in incorporating Reynolds number effects. One virtue of the model is that it can be directly related to Lagrangian statistics obtained from direct numerical simulations—which are found to depend strongly on Reynolds number. In the limit of infinite Reynolds number, the model reverts to the Langevin equation. [As Sawford shows, his model is equivalent to a different formulation given earlier by Krasnoff & Peskin (1971).]

As in Section 3 we consider stationary homogeneous isotropic turbulence with zero mean velocity. The turbulence is characterized by its intensity u' (or kinetic energy $k = \frac{3}{2}u'^2$), the mean dissipation rate $\langle\varepsilon\rangle$, and by the kinematic viscosity ν. In terms of these quantities, the Reynolds number is defined by:

$$Re = \frac{k^2}{\langle\varepsilon\rangle\nu}. \tag{72}$$

It is instructive to relate the Reynolds number to time scales. As usual, the eddy-turnover time T_E and the Kolmogorov time scale τ_η are defined by

$$T_E \equiv k/\langle\varepsilon\rangle = \tfrac{3}{2}u'^2/\langle\varepsilon\rangle, \tag{73}$$

and

$$\tau_\eta \equiv (\nu/\langle\varepsilon\rangle)^{1/2}. \tag{74}$$

Hence we obtain

$$Re = (T_E/\tau_\eta)^2. \tag{75}$$

The Langevin equation contains the single time scale T_E; whereas Sawford's stochastic model for acceleration contains two time scales, T_∞ and τ. These time scales (precisely defined below) scale as T_E and τ_η, respectively, at high Reynolds number.

Let $U^*(t)$ and $A^*(t)$ denote the model for one component of velocity and acceleration following a fluid particle. Then the velocity evolves by

$$\frac{d}{dt}U^*(t) = A^*(t). \tag{76}$$

With a'^2 defined by

$$a'^2 = u'^2/(T_\infty \tau), \tag{77}$$

Sawford's stochastic model for acceleration can be written

$$dA^*(t) = -\left\{1 + \frac{\tau}{T_\infty}A^*(t)\right\}\frac{dt}{\tau} - \frac{U^*(t)}{T_\infty}\frac{dt}{\tau} + \left\{2a'^2\left(1 + \frac{\tau}{T_\infty}\right)\right\}^{1/2} dW(t)/\tau^{1/2}, \tag{78}$$

where $W(t)$ is a Wiener process.

An analysis of this model (see Sawford 1991 or Priestly 1981) reveals that $U^*(t)$ and $A^*(t)$ are stationary processes with zero means and variances u'^2 and a'^2, respectively. The autocorrelation function of $U^*(t)$ is

$$\rho^*(s) = \left[e^{-|s|/T_\infty} - \left(\frac{\tau}{T_\infty}\right)e^{-|s|/\tau}\right] \Big/ \left(1 - \frac{\tau}{T_\infty}\right), \tag{79}$$

from which it follows that the (modeled) Lagrangian integral time scale is

$$T = T_\infty + \tau. \tag{80}$$

The principal features of this model are most clearly seen at high (but finite) Reynolds number, at which there is a complete separation of scales, i.e. $\tau \ll T_\infty$. For all times s much larger than τ, the velocity autocorrelation function is $\rho^*(s) \approx \exp(-|s|/T_\infty)$—the same as for the Langevin model. Consequently, in the inertial range ($\tau \ll s \ll T_\infty$), the Lagrangian velocity structure function varies linearly with s, in accord with the Kolmogorov hypotheses (Equations 25–27). Correspondingly, the Lagrangian velocity frequency spectrum varies as ω^{-2}. But for times s comparable to τ, this model is quite different from the Langevin model. Because $U^*(t)$ is a differentiable function of time, the autocorrelation function has zero slope at the origin. For not-too-large s/τ, the autocorrelation function of acceleration is $\rho_A^*(s) \approx \exp(-|s|/\tau)$. Correspondingly, the Lagrangian velocity frequency spectrum varies as ω^{-4} at high frequency ($\omega\tau \gg 1$).

In order to complete the model, two specifications are required to fix T_∞ and τ in terms of T_E and Re. Sawford (1991) used the Lagrangian DNS data of Yeung & Pope (1989) to achieve this. Here we do the same, but in a slightly different way. First, the DNS data on the Kolmogorov-scaled acceleration variance

$$a_o \equiv a'^2 \tau_\eta / \langle \varepsilon \rangle, \tag{81}$$

can be well approximated (for not too small R_λ) by

$$a_o \approx 3(1 - 22/R_\lambda), \tag{82}$$

where $R_\lambda = (20/3Re)^{1/2}$ is the Taylor-scale Reynolds number. [This form of correlation can be justified in terms of the inertial-range pressure fluctuation spectrum (M. S. Nelkin 1991, private communication; George et al 1984).] Second, for each value of R_λ studied in the DNS, the quantity

$$C_T(R_\lambda) \equiv \frac{4}{3} \frac{T_E}{T_\infty}, \tag{83}$$

can be determined by matching T/τ_η between DNS and the model. The values obtained are between 6 and 7, with a least-squares fit yielding

$$C_T \approx C_T(\infty)(1 + 4/R_\lambda), \tag{84}$$

with $C_T(\infty) = 6.2$. In this case there is no justification for the form of the correlation, and the data exhibit significant scatter around it. Given the empirical correlations for a_o and C_T the two time scales are determined as

$$T_\infty = T_E \left(\frac{4}{3C_T} \right), \tag{85}$$

and

$$\tau = \tau_\eta \left(\frac{C_T}{2a_o} \right). \tag{86}$$

The ability of this model to describe Lagrangian statistics is impressive. Figure 8 shows a comparison of the acceleration autocorrelation functions $\rho_A(s)$ obtained from the model and from DNS. The agreement indicates that the model provides a good approximation to the short-time behavior [although, because $A^*(t)$ is not differentiable, $\rho_A^*(s)$ has finite slope at the origin].

A revealing plot is of the Lagrangian velocity structure function $D_L(s)$ (Equation 25) normalized by $\langle \varepsilon \rangle s$. As may be seen from Figure 9, the model is in good agreement with the DNS data, and correctly shows that the peak value—denoted by C_0^*—increases with R_λ. According to the Kolmogorov hypotheses, at high Reynolds number, and for inertial-range times s ($\tau_\eta \ll s \ll T$), the quantity $D_L(s)/(\langle \varepsilon \rangle s)$, adopts a constant value C_0. It is readily shown that the model has this property, with $C_0 = C_T(\infty)$. But, as may be seen on Figure 10, the peak value C_0^* of $D_L(s)/(\langle \varepsilon \rangle s)$

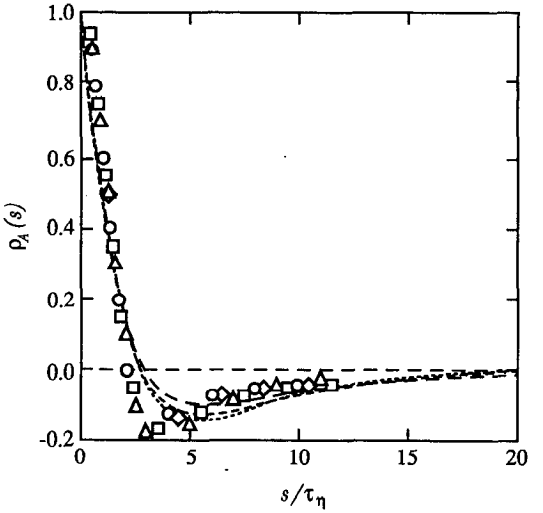

Figure 8 Acceleration autocorrelation function against Kolmogorov-scaled time lag. Symbols: DNS data (Yeung & Pope 1989); lines: Sawford's model. $R_\lambda = 38$: △ ---; $R_\lambda = 63$: □ – – –; $R_\lambda = 90$: ○ —·—; $R_\lambda = 93$: ◇. (From Sawford 1991, with permission.)

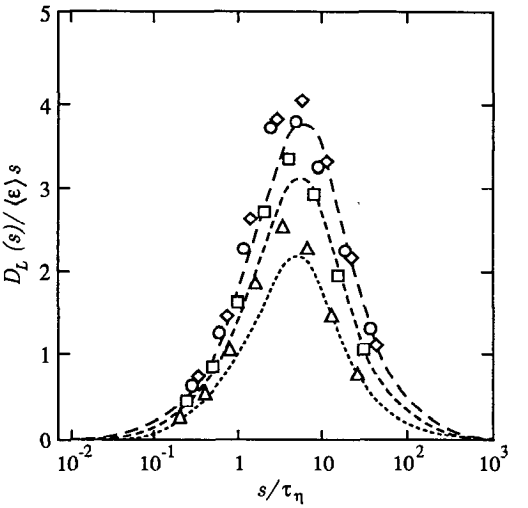

Figure 9 Lagrangian velocity structure function $D_L(s)$ divided by $\langle\varepsilon\rangle s$ against Kolmogorov-scaled time, s/τ_η. Symbols and lines, same as Figure 8. (From Sawford 1991, with permission.)

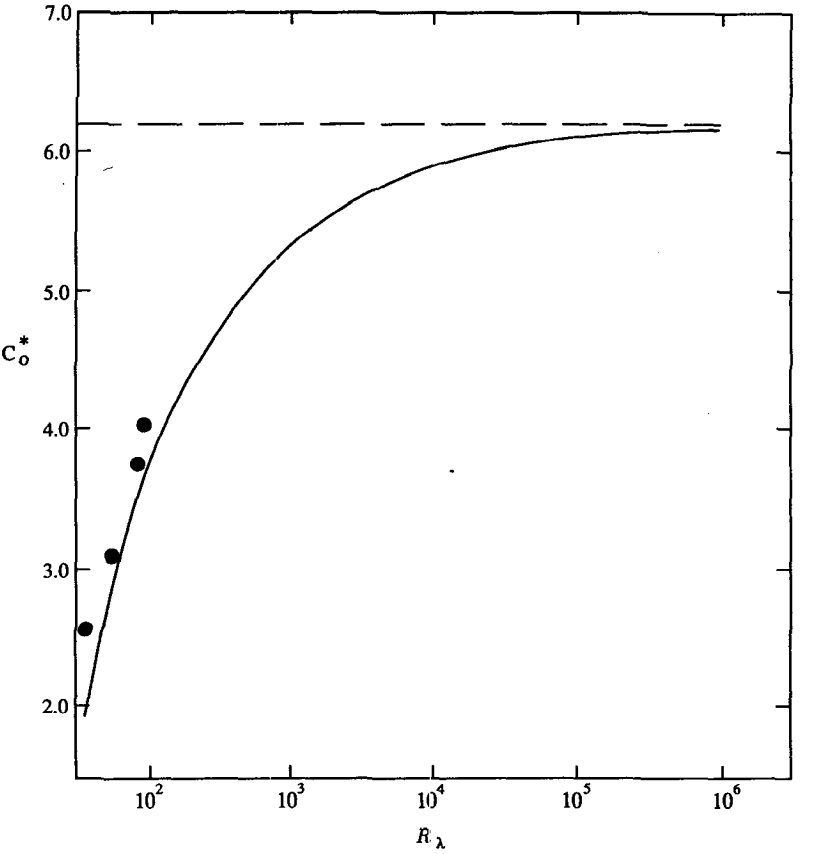

Figure 10 C_0^* [the peak value of $D_L(s)/\langle\varepsilon\rangle s$] against Taylor-scale Reynolds number. Symbols: DNS data (Yeung & Pope 1989); full line: from stochastic model for acceleration, dashed line: model asymptote $C_T(\infty)$.

approaches C_0 slowly as R_λ increases: At the relatively high value $R_\lambda = 1000$, C_0^* is only 85% of C_0.

Figure 11 shows the ratio of the Lagrangian to Eulerian time scales. It may be seen that this ratio varies appreciably over the range of R_λ accessible to DNS and wind tunnel experiments.

A question of some interest and importance is the value of the Kolmogorov constant C_0. The estimate from the above model [$C_0 = C_T(\infty) = 6.2$] is, in essence, obtained by extrapolating from DNS data in the R_λ range 40–90. Other values given in the literature are:

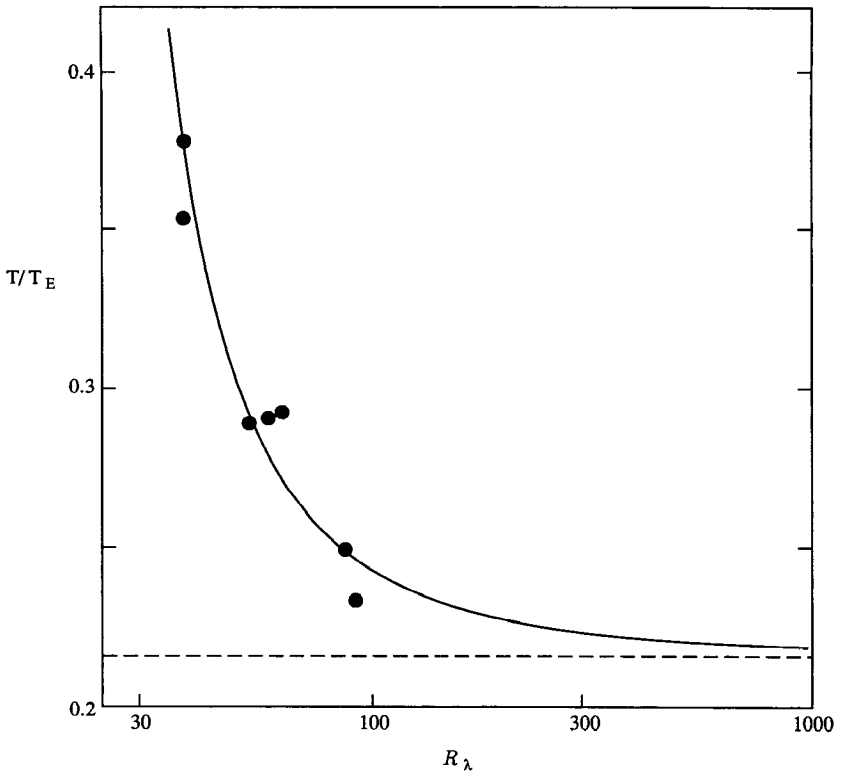

Figure 11 Ratio of Lagrangian to Eulerian time scales against Taylor-scale Reynolds number. Symbols: DNS (Yeung & Pope 1989); line: stochastic model for acceleration, Equations (83–86).

$C_0 \approx 3.8 \pm 1.9$ from measurements in the atmospheric boundary layer (Hanna 1981); $C_0 \approx 5.0$ from kinematic simulations (Fung et al 1992); $C_0 \approx 5.9$ from the Lagrangian renormalized approximation theory (Kaneda 1992); and $C_0 = 5.7$ based on the Langevin equation and further assumptions applied to the constant-stress region of the neutral atmospheric boundary layer (Rodean 1991). It is not unreasonable to suppose, therefore, that C_0 is in the range 5.0–6.5.

With the Langevin and refined Langevin models (which contain no Reynolds-number dependence) it is found that values of $C_0 = 2.1$ (Anand & Pope 1985) and $C_0 = 3.5$ (Pope & Chen 1990), respectively, are required to calculate accurately the dispersion behind a line source in grid turbulence at $R_\lambda \approx 70$. It is now apparent that these values—while being appropriate

values of the model constants at moderate Reynolds number—do not correspond to the value of the Kolmogorov constant C_0.

A stochastic model for the fluid particle acceleration $\mathbf{A}^*(t)$ (such as Equation 78), combined with the equations $\dot{\mathbf{x}}^* = \mathbf{U}^*$ and $\dot{\mathbf{U}}^* = \mathbf{A}^*$, leads to a modeled equation for the Eulerian joint pdf of velocity and acceleration, $f_{\mathbf{UA}}$. Such a model equation has not, to date, been applied to inhomogeneous flows. Compared to the velocity joint pdf equation (stemming from a Langevin equation), the equation for $f_{\mathbf{UA}}$ has the advantages of incorporating Reynolds-number effects and of representing Kolmogorov-scale processes. This may be of particular value in the study of near-wall flows.

5.5 *Other Stochastic Models*

Table 1 summarizes the stochastic Lagrangian models that have been proposed for various fluid properties.

Table 1 Stochastic Lagrangian models of turbulence

Subject of model	Authors
Fluid particle position	Taylor (1921)
Fluid particle velocity (single-particle dispersion)	Novikov (1963), Chung (1969), Frost (1975), Reid (1979), Wilson et al (1981a–c), Legg & Raupach (1982), Durbin (1983), Ley & Thomson (1983), Wilson et al (1983), Thomson (1984), Anand & Pope (1985), Van Dop et al (1985), De Baas et al (1986), Haworth & Pope (1986), Sawford (1986), Thomson (1986a), Pope (1987), Thomson (1987), MacInnes & Bracco (1992)
Fluid particle acceleration	Sawford (1991)
Relative velocity between fluid particle pairs (two-particle dispersion)	Novikov (1963), Durbin (1980), Lamb (1981), Gifford (1982), Sawford (1982), Durbin (1982), Lee & Stone (1983), Sawford & Hunt (1986), Thomson (1986b), Thomson (1990)
Dissipation	Pope & Chen (1990), Pope (1991b)
Velocity-gradient tensor	Pope & Cheng (1988), Girimaji & Pope (1990)
Scalar (e.g. species concentration)	Valiño & Dopazo (1991)
Scalar and scalar gradient	Fox (1992)

Taylor (1921) proposed a stochastic model for a component of fluid particle position $x^*(t)$ in which successive increments $\Delta x^* \equiv x^*(t+\Delta t) - x^*(t)$ are correlated. It is interesting to observe that the statistics implied by this model are identical to those from the Langevin equation (Durbin 1980).

For the fluid particle velocity $\mathbf{U}^*(t)$, early proposals for the use of the Langevin equation were made by Novikov (1963), Chung (1969), and Frost (1975). The works cited in Table 1 from the period 1979–1984 reflect active use of stochastic modeling of atmospheric dispersion. These models are essentially of the Langevin type, with the primary issue being the specification of the coefficients. In inhomogeneous flows, if the coefficients are specified incorrectly, stochastic models can predict (incorrectly) that an initially uniform distribution of particles becomes nonuniform. Most of the works since 1985 address this issue; a complete explanation is provided by Pope (1987).

The concentration variance of a contaminant in a turbulent flow can be studied in terms of the relative dispersion of fluid particle pairs (Batchelor 1952). Hence stochastic models have been developed (see Table 1) for the relative velocity between particles. These models have had some notable successes in predicting and explaining experimental observations. For example, Durbin (1982) shows that a two-particle dispersion model accounts for the observed sensitivity of the scalar variance in decaying grid turbulence to the initial scalar-to-velocity length scale ratio; and Thomson (1990) shows that his model accounts for the nontrivial evolution of the correlation coefficient between scalars emanating from a pair of line sources in grid turbulence, which has been studied experimentally by Warhaft (1984).

A key quantity in the specification of two-particle model coefficients is the separation distance between the particles. Only recently (Yeung 1993) have DNS results that can be used to develop and test such models become available. Some insight is also provided by kinematic simulations (Fung et al 1992).

The local deformation of material lines, surfaces, and volumes in a turbulent flow is determined by the velocity gradient tensor following the fluid (see e.g. Monin & Yaglom 1985). This motivated the development of stochastic Lagrangian models for the velocity gradient tensor by Pope & Cheng (1988) and Girimaji & Pope (1990). One use of such models is in the calculation of the area density of premixed turbulent flame sheets (Pope & Cheng 1988).

An important yet difficult topic is stochastic Lagrangian models $\boldsymbol{\phi}^*(t)$ for a set of scalars $\boldsymbol{\phi}^+(t)$—such as temperature and species concentrations. In conjunction with a Langevin model, a stochastic model for $\boldsymbol{\phi}^*(t)$ leads

to a modeled equation for the Eulerian joint pdf of velocity and composition which can be used to study turbulent reactive flows. Examples of applications of this approach can be found in Anand & Pope (1987), Masri & Pope (1990), Haworth & El Tahry (1991), Correa & Pope (1992), Noms (1993), Taing et al (1993), and elsewhere.

A set of compositions $\boldsymbol{\phi}$ has certain properties that are very different from these of velocity $\mathbf{U}$. Among these are: boundedness; localness of interactions in composition space; and (in important limiting cases) linearity and independence (Pope 1983b, 1985). These properties make the modeling of $\boldsymbol{\phi}^*(t)$ different and more difficult than the modeling of $\mathbf{U}^*(t)$. Currently there is no model that is even qualitatively satisfactory in all respects.

The simplest model—proposed in several different contexts and with different justifications—is the linear deterministic model:

$$\frac{d\boldsymbol{\phi}^*}{dt} = -C_\phi \langle \omega \rangle (\boldsymbol{\phi}^* - \langle \boldsymbol{\phi} \rangle) \tag{87}$$

(Chung 1969, Yamazaki & Ichigawa 1970, Dopazo & O'Brien 1974, Frost 1975, Borghi 1988). Although (in application to inhomogeneous turbulent reactive flows) the model is not without merit, because it is deterministic, it clearly provides a poor representation of time series of the fluid particle composition $\boldsymbol{\phi}^+(t)$.

Also widely employed are *stochastic mixing models* (e.g. Curl 1963, Dopazo 1979, Janicka et al 1979, Pope 1982). In the terminology of stochastic processes, these models are point processes: The value of $\boldsymbol{\phi}^*(t)$ is piecewise constant, changing discontinuously at discrete time points. Again, these models have their uses, but clearly the time series they generate, $\boldsymbol{\phi}^*(t)$, are qualitatively different to those of turbulent fluid, $\boldsymbol{\phi}^+(t)$.

Shown in Table 1 are the only proposed models that are stochastic, that generate continuous time series, and that preserve the boundedness of scalars. It is possible that a completely satisfactory model at this level will not be achieved. Instead, it may be necessary to incorporate more information, particularly that pertaining to scalar gradients (see e.g. Meyers & O'Brien 1981, Pope 1990, Fox 1992).

6. CONCLUSION

Lagrangian PDF methods are based on stochastic Lagrangian models—that is, stochastic models for the evolution of properties following fluid particles. For example, stochastic models for the fluid particle velocity $\mathbf{U}^*(t)$ (Equation 70) and for the turbulence frequency $\omega^*(t)$ (Equation 66)

lead to closed model equations for both the Lagrangian and Eulerian joint pdfs of these quantities. The Eulerian pdf equation can be used as a turbulence model to calculate the properties of inhomogeneous turbulence flows. This equation is solved numerically by a Monte Carlo method which is based, naturally, on the tracking of a large number of particles.

The primary stochastic models reviewed here are for velocity (based on the Langevin equation), for the turbulent frequency (or dissipation), and for the fluid particle acceleration. Lagrangian statistics extracted from direct numerical simulations of homogeneous turbulence have played a central role in the development of these models. Similar statistics at higher Reynolds numbers and in inhomogeneous flows are needed to develop and test the models further.

Other fluid properties—most importantly the composition ϕ—can be adjoined to the PDF method. This requires stochastic models for the quantities involved. In spite of considerable efforts, deficiencies remain in stochastic models for composition.

There is a close connection between Lagrangian PDF methods and Reynolds-stress closures. This connection can be used to benefit both approaches. In particular, new ideas in Reynolds-stress modeling (e.g. Durbin 1991, Lumley 1992, Reynolds 1992) can be readily incorporated in PDF methods.

ACKNOWLEDGMENTS

I am grateful to Dr. B. L. Sawford for permission to reproduce Figures 8 and 9.

For comments and suggestions on the draft of this paper I thank M. S. Anand, R. O. Fox, D. C. Haworth, J. C. R. Hunt, B. L. Sawford, D. J. Thomson, C. C. Volte, and P. K. Yeung.

This work was supported in part by the US Air Force Office of Scientific Research (grant number AFOSR-91-0184), and by the National Science Foundation (grant number CTS-9113236).

Literature Cited

Anand, M. S., Pope, S. B. 1985. Diffusion behind a line source in grid turbulence. In *Turbulent Shear Flows* 4, ed. L. J. S. Bradbury, F. Durst, B. E. Launder, F. W. Schmidt, J. H. Whitelaw, pp. 46–61. Berlin: Springer-Verlag

Anand, M. S., Pope, S. B. 1987. Calculations of premixed turbulent flames by pdf methods. *Combust. Flame* 67: 127–42

Anand, M. S., Pope, S. B., Mongia, H. C. 1989. A pdf method for turbulent recirculating flows. In *Turbulent Reactive Flows, Lect. Notes in Engrg.* 40: 672–93. Berlin: Springer-Verlag

Anand, M. S., Pope, S. B., Mongia, H. C. 1993. PDF calculations of swirling flows. *AIAA Pap. 93-0106*

Arnold, L. 1974. *Stochastic Differential Equations: Theory and Applications.* New York: Wiley. 228 pp.

Batchelor, G. K. 1952. Diffusion in a field of homogeneous turbulence. II The relative

motion of particles. *Proc. Cambridge Phil. Soc.* 48: 345–62
Bilger, R. W. 1980. Turbulent flows with nonpremixed reactants. In *Turbulent Reacting Flows*, ed. P. A. Libby, F. A. Williams, pp. 65–113. Berlin: Springer-Verlag
Billingsley, P. 1986. *Probability and Measure*. New York: Wiley. 622 pp.
Bockhorn, H. 1990. Sensitivity analysis based reduction of complex reaction mechanisms in turbulent non-premixed combustion. *Symp. (Int.) Combust.* 23*rd*, pp. 767–74. Pittsburgh: Combust. Inst.
Borghi, R. 1988. Turbulent combustion modelling. *Prog. Energy Combust. Sci.* 14: 245–92
Chen, H., Chen, S., Kraichnan, R. H. 1989. Probability distribution of a stochastically advected scalar field. *Phys. Rev. Lett.* 63: 2657–60
Chen, J.-Y., Dibble, R. W., Bilger, R. W. 1990. PDF modeling of turbulent nonpremixed $CO/H_2/N_2$ jet flames with reduced mechanisms. *Symp. (Int.) Combust.* 23*rd*, pp. 775–80. Pittsburgh: Combust. Inst.
Chung, P. M. 1969. A simplified statistical model of turbulent chemically reacting shear flows. *AIAA J.* 7: 1982–91
Correa, S. M., Drake, M, C., Pitz, R. W., Shyy, W. 1984. Prediction and measurement of a non-equilibrium turbulent diffusion flame. *Symp. (Int.) Combust.* 20*th*, pp. 337–43. Pittsburgh: Combust. Inst.
Correa, S. M., Pope, S. B. 1992. Comparison of a Monte Carlo PDF finite-volume mean flow model with bluff-body Raman data. *Symp. (Int.) Combust.* 24*th*, pp. 279–85. Pittsburgh: Combust. Inst.
Curl, R. L. 1963. Dispersed phase mixing: I. Theory and effects of simple reactors. *AIChE J.* 9: 175–81
Deardorff, J. W. 1978. Closure of second- and third-moment rate equations for diffusion in homogeneous turbulence. *Phys. Fluids* 21: 525–30
De Boas, A. F., Van Dop, H., Nieuwstadt, F. T. M. 1986. An application of the Langevin equation for inhomogeneous conditions to dispersion in a convective boundary layer. *Q. J. R. Meteorol. Soc.* 112: 165–80
Dopazo, C. 1979. Relaxation of initial probability density functions in the turbulent convection of scalar fields. *Phys. Fluids* 22: 20–30
Dopazo, C. 1993. Recent developments in PDF methods. In *Turbulent Reacting Flows*, ed. P. A. Libby, F. A. Williams. New York: Academic. In press
Dopazo, C., O'Brien, E. E. 1974. An approach to the autoignition of a turbulent mixture. *Acta Astronaut.* 1: 1239–66
Durbin, P. A. 1980. A stochastic model of two-particle dispersion and concentration fluctuations in homogeneous turbulence. *J. Fluid Mech.* 100: 279–302
Durbin, P. A. 1982. Analysis of the decay of temperature fluctuations in isotropic turbulence. *Phys. Fluids* 25: 1328–32
Durbin, P. A. 1983. Stochastic Differential Equations and Turbulent Dispersion. *NASA Ref Publ.* 1103
Durbin, P. A. 1991.*Theoret. Comput. Fluid Dyn.*3: 1–13
Eubank, R. L. 1988. *Spline Smoothing and Nonparametric Regression*. New York: Marcel Dekker. 438 pp.
Fox, R. O. 1992. The Fokker-Planck closure for turbulent molecular mixing: passive scalars. *Phys. Fluids A* 4: 1230–44
Frost, V. A. 1975. Model of a turbulent, diffusion-controlled flame jet. *Fluid Mech. Sov. Res.* 4: 124–33
Fung, J. C. H., Hunt, J. C. R., Malik, N. A., Perkins, R. J. 1992. Kinematic simulation of homogeneous turbulence by unsteady random Fourier modes. *J. Fluid Mech.* 236: 28 1–83
Gao, F. 1991. Mapping closure and non-Gaussianity of the scalar probability density function in isotropic turbulence. *Phys. Fluids A* 3: 2438–44
Gao, F., O'Brien, E. E. 1991. A mapping closure for multispecies Fickian diffusion. *Phys. Fluids A* 3: 956–59
Gardiner, C. W. 1990. *Handbook of Stochastic Methods for Physics Chemistry and Natural Sciences*. Berlin: Springer-Verlag. 442 pp. 2nd ed.
Gence, J. N., Mathieu, J. 1979. On the application of successive plane strains to grid-generated turbulence. *J. Fluid Mech.* 93: 501–13
George, W. K., Beuther, P. D., Arndt, R. E. A. 1984. Pressure spectra in turbulent free shear flows. *J. Fluid Mech.* 148: 155–91
Gifford, F. A. 1982. Horizontal diffusion in the atmosphere: a Lagrangian dynamical theory. *Atmos. Environ.* 16: 505–12
Girimaji, S. S. 1991. Assumed β-pdf model for turbulent mixing: validation and extension to multiple scalar mixing. *Combust. Sci. Technol.* 78: 177–96
Girimaji, S. S., Pope, S. B. 1990. A stochastic model for velocity gradients in turbulence. *Phys. Fluids A* 2: 242–56
Hanna, S. R. 1981. Lagrangian and Eulerian time-scale relation in the daytime boundary layer. *J. Appl. Meteorol.* 20: 242–49
Härdle, W. 1990. *Applied Nonparameteric Regression*. Cambridge: Cambridge Univ. Press. 333 pp.

Haworth, D. C., El Tahry, S. H. 1991. Probability density function approach for multidimensional turbulent flow calculations with application to in-cylinder flows in reciprocating engines. *AIAA J.* 29: 208–18

Haworth, D. C., Pope, S. B. 1986. A generalized Langevin model for turbulent flows. *Phys. Fluids* 29: 387–405

Haworth, D. C., Pope, S. B. 1987. A pdf modelling study of self-similar turbulent free shear flow. *Phys. Fluids* 30: 1026–44

Janicka, J., Kolbe, W., Kollmann, W. 1977. Closure of the transport equation for the probability density function of turbulent scalar fields. *J. Non-equilib. Thermodyn.* 4: 47–66

Kaneda, Y. 1993. Lagangian and Eulerian time correlations in turbulence. Submitted

Kolmogorov, A. N. 1941. Local structure of turbulence in an incompressible fluid at very high Reynolds numbers. *Dokl. Akad. Nauk SSSR* 30: 299–303

Kolmogorov, A. N. 1942. Equations of turbulent motion of an incompressible fluid. *Izv. Acad. Sci. USSR Phys.* 6: 56–58

Kolmogorov, A. N. 1962. A refinement of previous hypotheses concerning the local structure of turbulence in a viscous incompressible fluid at high Reynolds number. *J. Fluid Mech.* 13: 82–85

Krasnoff, E., Peskin, R. L. 1971. The Langevin model for turbulent diffusion. *Geophys. Fluid Dyn.* 2: 123–46

Kuznetsov, V. R., Sabel'nikov, V. A. 1990. *Turbulence and Combustion.* New York: Hemisphere. 362 pp.

Lamb, R. G. 198 1. A scheme for simulating particle pair motions in turbulent fluid. *J. Comput. Phys.* 39: 329–46

Lang, D. B. 1985. *Laser Doppler velocity and vorticity measurements in turbulent shear layers.* PhD thesis. Calif. Inst. Technol.

Launder, B. E., Spalding, D. B. 1972. *Mathematical Models of Turbulence.* New York: Academic

Lee, J. T., Stone, G. L. 1983. The use of Eulerian initial conditions in a Lagrangian model of turbulent diffusion. *Atmos. Environ.* 17: 2477–81

Legg, B. J., Raupach, M. R. 1982. Markov-chain simulation of particle dispersion in inhomogeneous flows: the mean drift velocity induced by a gradient in the Eulerian velocity variance. *Boundary-Layer Meteorol.* 24: 3–13

Ley, A. J., Thomson, D. J. 1983. A random walk model of dispersion in the diabatic surface layer. *Q. J. R. Meteorol. Soc.* 109: 867–80

Lockwood, F. C., Naguib, A. S. 1975. The prediction of the fluctuations in the properties of free, round jet, turbulent, diffusion flames. *Combust. Flame* 24: 109–24

Lumley, J. L. 1992. Some comments on turbulence. *Phys. Fluids A* 4: 203–11

MacInnes, J. M., Bracco, F. V. 1992. Stochastic particle dispersion modeling and the tracer-particle limit. *Phys. Fluids A* 4: 2809–24

Masri, A. R., Pope, S. B. 1990. PDF calculations of piloted turbulent non-premixed flames of methane. *Combust. Flame* 81: 13–29

Meyers, R. E., O'Brien, E. E. 1981. The joint pdf of a scalar and its gradient at a point in a turbulent fluid. *Combust. Sci. Technol.* 26: 123–34

Monin, A. S., Yaglom, A. M. 1975. *Statistical Fluid Mechanics,* Vol. 2. Cambridge, Mass: MIT Press. 874 pp.

Naot, D., Shavit, A., Wolfshtein, M. 1970. Interactions between components of the turbulent velocity correlation tensor due to pressure fluctuations. *Israel J. Technol.* 8: 259–69

Norris, A. T. 1993. *The application of PDF methods to piloted diffusion flames.* PhD thesis, Cornell Univ.

Novikov, E. A. 1963. Random force method in turbulence theory. *Sov. Phys. JETP* 17: 1449–54

Pope, S. B., 1980. Probability distributions of scalars in turbulent shear flows. In *Turbulent Shear Flows* 2, ed. L. J. S. Bradbury, F. Durst, B. E. Launder, F. W. Schmidt, J. H. Whitelaw, pp. 7–16. Berlin: Springer-Verlag

Pope, S. B., 1982. An improved turbulent mixing model. *Combust. Sci. Technol.* 28: 13 1–45

Pope, S. B. 1983a. A Lagrangian two-time probability density function equation for inhomogeneous turbulent flows. *Phys. Fluids* 26: 3448–50

Pope, S. B. 1983b. Consistent modeling of scalars in turbulent flows. *Phys. Fluids* 26: 404–8

Pope, S. B. 1985. PDF methods for turbulent reactive flows. *Prog. Energy Combust. Sci.* 11: 119–92

Pope, S. B. 1987. Consistency conditions for random-walk models of turbulent dispersion. *Phys. Fluids* 30: 2374–79

Pope, S. B. 1990. Computations of turbulent combustion: progress and challenges. *Symp. (Int.) Combust.* 23*rd*, pp. 591–612. Pittsburgh: Combust. Inst.

Pope, S. B. 1991a. Mapping closures for turbulent mixing and reaction. *Theoret. Comput. Fluid Dyn.* 2: 255–70

Pope, S. B. 1991b. Application of the velocity-dissipation probability density function model to inhomogeneous turbulent

flows. *Phys. Fluids A* 3: 1947–57 (See also Erratum: *Phys. Fluids A* 1992. 4: 1088)
Pope, S. B. 1993. On the relationship between stochastic Lagrangian models of turbulence and second-moment closures. *Phys. Fluids A*. 2: to be published
Pope, S. B., Chen, Y. L. 1990. The velocity-dissipation probability density function model for turbulent flows. *Phys. Fluids A* 2: 1437–49
Pope, S. B., Cheng, W. K. 1988. Statistical calculations of spherical turbulent flames. *Symp. (Int.) Combust. 21st*, pp. 1473–82. Pittsburgh: Combust. Inst.
Pope, S. B., Ching, E. S. C. 1993. Stationary probability density functions in turbulence. *Phys. Fluids A*. In press
Priestley, M. B. 1981. *Spectral Analysis and Time Series*. New York: Academic
Reid, J. D. 1979. Markov chain simulations of vertical dispersion in the neutral surface layer for surface and elevated releases. *Boundary-Layer Meteorol.* 16: 3–22
Reynolds, W. C. 1990. The potential and limitations of direct and large eddy simulations. In *Whither Turbulence? Turbulence at the Crossroads*, ed. J. L. Lumley, pp. 313–43. Berlin: Springer-Verlag
Reynolds, W. C. 1992. Towards a structure-based turbulence model. *Bull. Am. Phys. Soc.* 37: 1727
Rhodes, R. P. 1975. A probability distribution function for turbulent flows. In *Turbulent Mixing in Nonreactive and Reactive Flows*, ed. S. N. B. Murthy, pp. 235–41. New York/London: Plenum. 464 pp.
Risken, H. 1989. *The Fokker-Planck Equation: Methods of Solution and Applications*. Berlin: Springer-Verlag. 472 pp. 2nd ed.
Rodean, H. C. 1991. The universal constant for the Lagrangian structure function. *Phys. Fluids A* 3: 1479–80
Roekaerts, D. 1991. Use of a Monte Carlo PDF method in a study of the influence of turbulent fluctuations on selectivity in a jet-stirred reactor. *Appl. Sci. Res.* 48: 271–300
Rotta, J. C. 195 1. Statistische Theorie nichthomogener Turbulenz. *Z. Phys.* 129: 547–72
Sawford, B. L. 1982. Lagrangian Monte Carlo simulation of the turbulent motion of a pair of particles. *Q. J. R. Meteorol. Soc.* 108: 207–13
Sawford, B. L. 1986. Generalized random forcing in random-walk turbulent dispersion models. *Phys. Fluids* 29: 3582–85
Sawford, B. L., Hunt, J. C. R. 1986. Effects of turbulence structure, molecular diffusion and source size on scalar fluctuations in homogeneous turbulence. *J. Fluid Mech.* 165: 373–400
Sawford, B. L. 1991. Reynolds number effects in Lagrangian stochastic models of turbulent dispersion. *Phys. Fluids A* 3: 1577–86
Silverman, B. W. 1986. *Density Estimation for Statistics and Data Analysis*. New York: Chapman and Hall
Sinai, Ya. G., Yakhot, V. 1989. Limiting probability distribution of a passive scalar in a random velocity field. *Phys. Rev. Lett.* 63: 1962–64
Speziale, C. G., Sarkar, S., Gatski, T. B. 1991. Modeling the pressure-strain correlation of turbulence: an invariant dynamical systems approach. *J. Fluid Mech.* 227: 245–72
Taing. S., Masri, A. R., Pope, S. B. 1993. PDF calculations of turbulent nonpremixed flames of H_2/CO_2 using reduced chemical mechanisms. *Combust. Flame* In press
Tapia, R. A., Thompson, J. R. 1978. *Nonparametric Density Estimation*. Baltimore: Johns Hopkins Press
Tavoularis, S., Corrsin, S. 1981. Experiments in nearly homogeneous turbulent shear flow with a uniform mean temperature gradient. Part 1. *J. Fluid Mech.* 104: 311–47
Taylor, G. I. 1921. Diffusion by continuous movements. *Proc. London Math. Soc.* 20: 196–212
Thomson, D. J. 1984. Random walk modelling of diffusion in inhomogeneous turbulence. *Q. J. R. Meteorol. Soc.* 110: 1107–20
Thomson, D. J. 1986a. A random walk model of dispersion in turbulent flows and its application to dispersion in a valley. *Q. J. R. Meteorol. Soc.* 112: 511–30
Thomson, D. J. 1986b. On the relative dispersion of two particles in homogeneous stationary turbulence and the implications for the size of the concentration fluctuations at large times. *Q. J. R. Meteorol. Soc.* 112: 890–94
Thomson, D. J. 1987. Criteria for the selection of stochastic models of particle trajectories in turbulent flows. *J. Fluid Mech.* 180: 529–56
Thomson, D. J. 1990. A stochastic model for the motion of particle pairs in isotropic high-Reynolds-number turbulence, and its application to the problem of concentration variance. *J. Fluid Mech.* 210: 113–53
Valiño, L., Dopazo, C. 1991. A binomial Langevin model for turbulent mixing. *Phys. Fluids A* 3: 3034–37
Van Dop, H., Nieuwstadt, F. T. M., Hunt, J. C. R. 1985. Random walk models for particle displacements in inhomogeneous unsteady turbulent flows. *Phys. Fluids* 28: 1639–53

van Kampen, N. G. 1981. *Stochastic Processes in Physics and Chemistry*. Amsterdam: North-Holland

Wilcox, D. C. 1988. Multiscale model for turbulent flows. *AIAA J.* 26: 1311–20

Wilson, J. D., Thurtell, G. W., Kidd, G. E. 1981a. Numerical simulation of particle trajectories in inhomogeneous turbulence, I: Systems with constant turbulent velocity scale. *Boundary-Layer Meteorol.* 21: 295–313

Wilson, J. D., Thurtell, G. W., Kidd, G. E. 1981b. Numerical simulation of particle trajectories in inhomogeneous turbulence, II: Systems with variable turbulent velocity scale. *Boundary-Layer Meteorol.* 21: 423–41

Wilson, J. D., Thurtell, G. W., Kidd, G. E. 1981c. Numerical simulation of particle trajectories in inhomogeneous turbulence, III: Comparion of predictions with experimental data for the atmospheric surface layer. *Boundary-Layer Meteorol.* 21: 443–63

Wilson, J. D., Legg, B. J., Thomson, D. J. 1983. Calculation of particle trajectories in the presence of a gradient in turbulent-velocity variance. *Boundary-Layer Meteorol.* 27: 163–69

Yamazaki, H., Ichigawa, A. 1970. *Int. Chem. Eng.* 10: 471–78

Yeung, P. K. 1993. Direct numerical simulation of relative diffusion in stationary isotropic turbulence. *Ninth Symp. in Turbulent Shear Flows*, Kyoto, Japan

Yeung, P. K., Pope, S. B. 1989. Lagrangian statistics from direct numerical simulations of isotropic turbulence. *J. Fluid Mech.* 207: 531–86